Changes in the nutrient inputs to global coastal zones and implications for algal blooms in the 21st century

By Fatemeh Afsari (8897530)

A Project from Utrecht University

Canada's west coast

First supervisor: Jack Middelburg

Second supervisor: Junjie Wang

Utrecht University

Acknowledgments

I'm grateful for the opportunity to work on this project at Utrecht University (UU). I want to thank my supervisors, Jack Middelburg and Junjie Wang, for their invaluable support. Many thanks to my friends for their assistance as well.

Abstract

Over the past decades, the delivery of nutrients particularly nitrogen (N) and phosphorus (P) from land to river basins has increased due to human activities such as intensified agriculture and increased wastewater discharge. River nutrient export to oceans has risen alongside contributions from atmospheric deposition, submarine fresh groundwater discharge, and mariculture. This study used a combination of the process-based Integrated Model to Assess the Global Environment-Global Nutrient Model (IMAGE-GNM), atmospheric deposition models (TM5-FASST and CAM4), and remote-sensing data to quantify changes in external N and P inputs from river export, atmospheric deposition, submarine fresh groundwater discharge, and mariculture to global coastal zones over the past two decades, as well as their potential impacts on the evolution of global coastal algal blooms. The total nitrogen (TN) and phosphorus (TP) inputs from river export, atmospheric deposition, submarine fresh groundwater discharge, and mariculture showed an increase in most large marine ecosystems (LMEs). Overall river export and atmospheric deposition were the main contributors, collectively contributing 85-100% to the TN inputs and 62-100% to the TP inputs to global LMEs on average during the period from 2000 to 2015. The main sources of TN and TP in river export are anthropogenic in 32 and 34 LMEs, respectively, and are related to agricultural activities, wastewater discharge, and aquaculture. For all LMEs, the average contributions of anthropogenic sources to river export of TN and TP were about 56% and 57%, respectively. The TN inputs increased in 33 LMEs, stayed stably high in 21 LMEs, and decreased only in 8 LMEs. The TP input increased in 32 LMEs, stayed stable in 17 LMEs, and decreased only in 13 LMEs. In most (about 80% of) LMEs, the molar TN: TP ratios of nutrient inputs were above the Redfield ratio (N:P=16) during 2000-2015, and 18 LMEs showed increases in their TN:TP ratios in nutrient inputs during this period. In about half of the global LMEs, the coastal algal bloom frequency and the molar TN:TP ratio in nutrient inputs showed a positive correlation relationship. The rest LMEs showed no positive correlations between the coastal algal bloom frequency and the molar TN: TP ratio in nutrient inputs, but the coastal algal blooms in most of these LMEs occurred with the molar TN: TP ratio in nutrient inputs exceeding the Redfield ratio. Rising N and P inputs to global coastal waters with imbalanced ratios may have posed elevated risks of coastal harmful algal blooms, which negatively influence biodiversity, water quality, fishing resources and the economy. Measures that reduce nutrient loads and account for nutrient ratios should be taken to control coastal algal blooms.

Index

1. Introduction

Nutrients are crucial in sustaining life and food production. During the past decades, there has been a noteworthy increase in the transport of nutrients of nitrogen (N) and phosphorus (P) from terrestrial systems to river basins, due to human activities such as intensified and expanded agriculture and increased wastewater discharge (Beusen et al., 2016). As a result, nutrient export from rivers to oceans has increased. Meanwhile, coastal seas also receive nutrient inputs from atmospheric deposition, submarine fresh groundwater discharge, and mariculture. The excessive inputs of N and P into global coastal waters may cause eutrophication and trigger a cascade of environmental issues, including harmful algal blooms (HABs) (Anderson et al., 2002), biodiversity loss (Rabalais, 2002), hypoxia (Vaquer-Sunyer, 2008), and adverse impacts on fishing resources and local economies (Hallegraeff, 1993). Moreover, the elevated nutrient inputs may also cause imbalanced ratios of nutrients in coastal waters compared to the phytoplankton nutrient uptake ratio, i.e., the Redfield molar ratio of N: P=16:1 (Zhou, 2023). The elevated nutrient inputs together with imbalanced nutrient ratios may promote the preferential growth of specific algal species, resulting in algal blooms, which are usually harmful or even toxic (Glibert, 2020; Wang et al., 2021). Moreover, the causes of HAB proliferation are intricate, influenced not only by nutrient quantities and stoichiometry but also by factors like hydrodynamic conditions, water column circulation, and climate (Diaz et al., 2008). The complexity of these compound impacts makes the relationship between algal blooms and nutrient inputs elusive (Glibert, 2020).

Previous research has brought to light the crucial role played by rising nutrient inputs of N and P in triggering HABs (Wang et al., 2020a; Wang et al., 2021; Wang et al., 2023). However, studies have often been confined to specific regions, such as Chinese coastal waters by Wang et al. (2021) and Wang et al. (2023), and north of Europe by Karlson et al. (2021). Moreover, the long-term trends of nutrients and algal blooms are rarely compared in the same way due to data limitations in nutrients and/or algal blooms in each system. These limitations restrict insights into the temporal and spatial variability of the relationship between nutrient inputs and HABs.

While some European countries have developed policies and initiated actions to reduce nutrient loads to improve water quality in recent decades, other countries, particularly those in the developing world, lack such measures and still have increased nutrient loads, often due to low nutrient use efficiencies and low wastewater treatment abilities. As a result, the nutrient inputs to different coastal systems may change differently over the recent decades and pose different impacts on the local HAB development. It is therefore crucial to understand the temporal changes in the external nutrient inputs and their ratios from various sources to global oceans. This understanding should encompass alterations in human activities across different regions and countries over the past two decades. Moreover, analyzing the relationship between the temporal changes in external nutrient inputs and coastal algal blooms on a global and regional scale can enhance our standing of the role of nutrients in HAB development, provide suggestions for water quality improvement, prevent future HABs, and mitigate negative effects on coastal organisms and ecosystems.

This study aims to explore the long-term spatial-temporal changes in external N and P inputs to global coastal oceans in the 21st century and their potential implications for coastal algal blooms. The research employs an integrated approach, combining the process-based models of the Integrated Model to Assess the Global Environment-Global Nutrient Model (IMAGE-GNM) (Beusen et al., 2015), IMAGE-GNM aquaculture nutrient budget model (Wang et al., 2020b), atmospheric deposition models (TM5-FASST) by Van Dingenen et al. (2018) and (CAM4) by Brahney et al. (2015), and remote-sensing data from Dai et al. (2023). Using a coupling of these models and data, the temporal changes in the annual fluxes of external N and P inputs to global Large Marine Ecosystems (LMEs) from river export, atmospheric deposition, submarine fresh

groundwater discharge, and mariculture from 2000 to 2015 are quantified. By comparing the changes in the total external nutrient inputs and ratios with the remote-sensing-based algal bloom frequency data, the potential impacts of nutrient changes on the evolution of global coastal algal blooms are assessed.

2. Research question

- How much are the nutrient (N and P) inputs to the coastal waters of different global LMEs and how do they change from 2000 to 2015?
- What are the contributions of different sources to the external N and P inputs, how do they change, and which source(s) are dominant for different LMEs?
- What are the potential relationships between the molar N:P ratios in nutrient inputs and the coastal algal bloom frequencies across different LMEs?

3. Materials and methods

3.1 Quantifying Nutrient Loadings to Coastal Waters

In this study, the external N inputs to each LME include river export, submarine fresh groundwater discharge, mariculture, and atmospheric deposition (Figure 1). The external P inputs to each LME include river export, mariculture, and atmospheric deposition (Figure 1). Various nutrient sources to rivers, riverine nutrient export, and submarine fresh groundwater N discharge to global LMEs were simulated using IMAGE-GNM (Beusen et al., 2015). N and P release from mariculture was simulated using the IMAGE-GNM aquaculture nutrient budget model (Wang et al., 2020b). Atmospheric N deposition was simulated using the TM5-FAst Scenario Screening Tool (TM5-FASST) model (Van Dingenen et al., 2018). Atmospheric P deposition was simulated using the Community Atmospheric Model (CAM4) (Brahney et al., 2015).

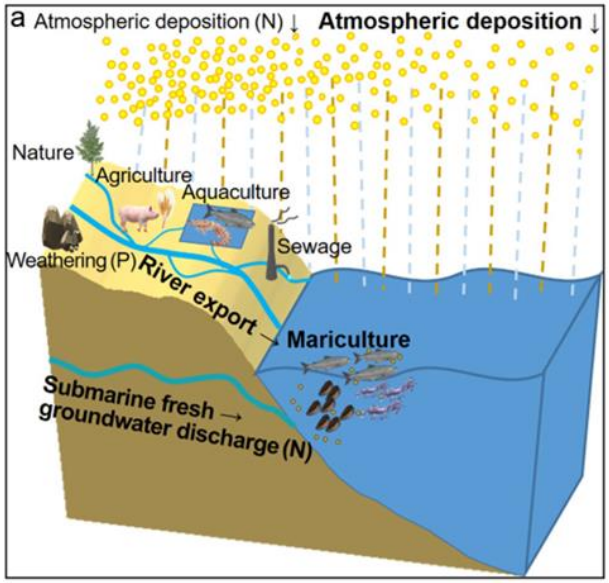

Figure 1. The conceptual model of estimating external nitrogen and phosphorus inputs to coastal waters, cited from Wang et al., (2021).

3.2 Nutrients from River Export and Submarine Fresh Groundwater Discharge

IMAGE-GNM is a global spatially explicit, integrated assessment model for simulating nutrient delivery from all known natural and anthropogenic sources to river basins and their transport along the river to coastal waters at a spatial resolution of 0.5 by 0.5 degree (Beusen et al., 2015) (Figure 2). IMAGE-GNM couples the data of land use, climate, and human activities simulated by IMAGE (Stehfest et al., 2014) with the PCR-GLOBWB hydrological model (Van Beek et al., 2011), which simulated water balance, runoff, and discharge in global river basins.

IMAGE-GNM includes N and P delivery from agricultural and natural land systems (i.e., N and P via runoff to surface water and N via leaching through shallow and deep groundwater, riparian zones, and finally to surface water), wastewater discharge, aquaculture and allochthonous organic material from vegetation in floodplains, N delivery from atmospheric deposition to terrestrial surfaces and waterbodies and P delivery from weathering (Figure 2). Each grid cell receives water containing N and P from upstream and diffuse/point sources within the cell. IMAGE-GNM uses the nutrient-spiraling ecological concept to calculate in-stream retention (Beusen et al., 2015). After in-stream retention is considered, water and nutrients are transported to downstream grid cells. Discharge is routed to determine the cumulative water and nutrient flux in each grid cell, covering rivers, lakes, wetlands, and reservoirs (Figure 1c). A more detailed description of IMAGE-GNM can be found in Beusen et al. (2015).

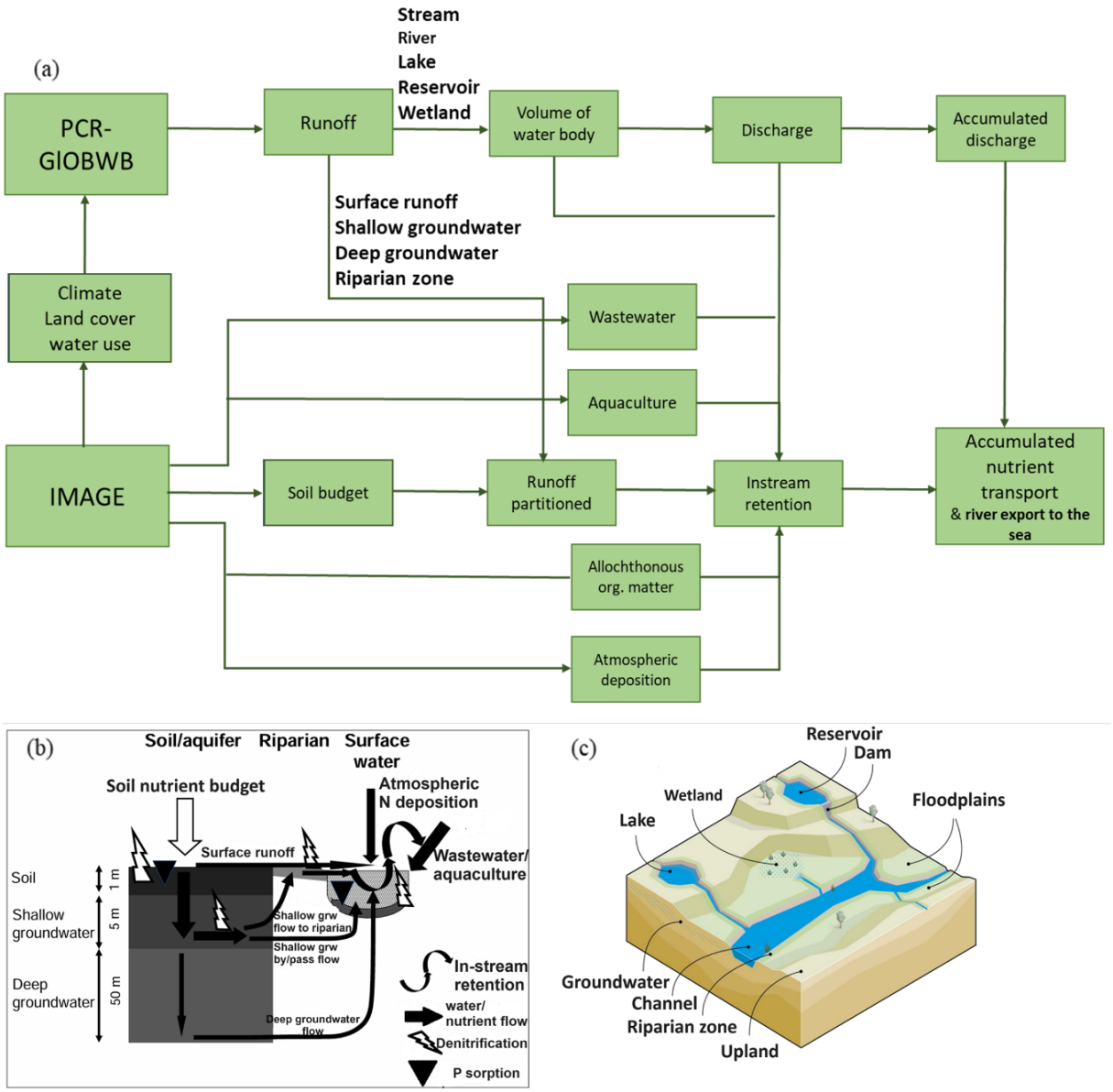

Figure 2. (a) Scheme of the IMAGE-GNM model framework which couples river hydrology simulated by PCR-GLOBWB model (Van Beek et al., 2011) and human activities simulated by IMAGE model (Stehfest et al., 2014), modified from Beusen et al. (2015). (b) Scheme of the flows of water and nutrients, and retention processes within a grid cell, modified from Beusen et al. (2015). (c) Scheme of the flow of water (containing nitrogen and phosphorus) in a landscape featuring streams, rivers, lakes, wetlands, and reservoirs, modified from Beusen et al. (2015).

3.3 Nitrogen Release from Mariculture

N and P release from mariculture (and freshwater aquaculture) was evaluated using the IMAGE-GNM aquaculture nutrient budget model based on annual mariculture (and freshwater aquaculture) production data from FISHSTAT (FAO, 2021; Wang et al., 2020b). The spatial distribution of coastal mariculture

considers parameters such as coastline length and temperature, as outlined by Wang et al. (2020b). More details about this model can be found in Bouwman et al. (2011) and Bouwman et al. (2013).

3.4 Atmospheric nutrient deposition

3.4.1 Atmospheric N deposition

TM5-FASST is a global reduced-form air quality source-receptor mode, which is specifically designed for analyzing the impacts of emission changes on air quality and short-lived climate pollutants with a 1 by 1-degree resolution (Van Dingenen et al., 2018). In conjunction with TM5, which is a 3-dimensional global atmospheric chemical transport model, TM5-FASST contributes significantly to simulating the transport, chemical processes, and both wet and dry deposition of chemically active atmospheric trace gases. These gases encompass ozone (O_3), sulfur dioxide (SO_2), nitrogen oxides (NO_x), volatile organic compounds (VOCs), and ammonia (NH_3), along with various particulate matter components such as sulfate (SO_4^{2-}), nitrate (NO_3^-), ammonium (NH_4^+), primary PM2.5, and its constituents, including black carbon, organic carbon, sea salt, and mineral dust.

The national data on NO_x and NH_3 emissions from the Edgar (2019) dataset were aggregated into 56 regional levels to drive the TM5-FASST model. The primary constituents considered for total N are NO_x and NH_3. To obtain the total N concentration from atmospheric deposition, we sum the simulated concentrations of NO_x and NH_3. Subsequently, the data underwent interpolation to achieve a resolution of 0.5 by 0.5 degrees.

3.4.2 Atmospheric P deposition

Community Atmospheric Model (CAM4) (Brahney et al., 2015) with a spatial resolution of 2 by 2 degrees is used for estimating atmospheric P deposition. Atmospheric P deposition onto coastal grid cells was converted to the same 0.5 by 0.5-degree resolution.

3.5 Sources of global coastal algal bloom frequency data

To compare the molar TN:TP ratios in the external nutrient inputs to LMEs with the development of their coastal algal blooms, the remote-sensing based data of annual frequencies of global coastal algal blooms during the period 2003-2015 from Dai et al. (2023) are used. The data has an original 1x1km spatial resolution, and were transformed to regional coastal algal bloom frequencies in each LME following the method defined in Dai et al. (2023).

4. Results

4.1 Nitrogen input

The TN inputs increased in 33 LMEs, stayed stably high in 21 LMEs, and decreased only in 8 LMEs (Figures 3-8). For most LMEs, river export and atmospheric deposition play significant roles as N sources, totally accounting for 85-100% during 2000-2015 across all LMEs. The contributions of submarine fresh groundwater discharge and mariculture are minor and sometimes negligible. Mariculture plays a relatively more important role in the LMEs of the Barents Sea (20), the Norwegian Sea (21), the Faroe Plateau (60), the Gulf of Thailand (35), the South China Sea (36), the Indonesian Sea (38), the East China Sea (47), the Mediterranean Sea (26), the Northwest Australian Shelf (45), and the Pacific Central-American Coastal (11), than in other LMEs.

4.1.1 LMEs with increasing trends in total external N inputs during 2000-2015

Thirty-three LMEs showed increasing total external N inputs from all four sources during 2000-2015 (Figures 3-4). In these LMEs, river N export showed a substantial increase and atmospheric deposition slightly increased. These LMEs include the East Bering Sea (1), the Gulf of Alaska (2), the Gulf of California (4), the Pacific Central-American Coastal (11), the Patagonian Shelf (14), the South Brazil Shelf (15), the East Brazil Shelf (16), the Canary Current (27), the Guinea Current (28), the Benguela Current(29), the Somali Coastal Current (31), the Arabian Sea (32), the Red Sea (33), the Bay of Bengal (34), the Gulf of Thailand (35), the South China Sea (36), the Indonesian Sea (38), the Northeast Australian Shelf (40), the East Central Australian Shelf (41), the Southeast Australian Shelf (42), the South West Australian Shelf (43), the West Central Australian Shelf (44), the New Zealand Shelf (46), the East China Sea (47), the Yellow Sea (48), Kuroshio Current (49), the Sea of Japan (50), the Oyashio Current (51), the Sea of Okhotsk (52), the West Bering Sea (53), the Northern Bering - Chukchi Seas (54), the East Siberian Sea (56), and the Black Sea (62) (Figure 3-4).

Nineteen LMEs showed an increasing trend in their total external N inputs from 2000 to 2015 dominated by river export (Figure 3). For example, in the Bay of Bengal (34), there was an increase in the total external N inputs of 3829 Gg/yr from 2000 to 2015, with an average proportion of 65% from river export, 34% from atmospheric deposition, and 1% from mariculture and submarine fresh groundwater discharge during this period. In the Yellow Sea (48), the total external N inputs increased by 3572 Gg/yr from 2000 to 2015, with an average contribution of 89% from river export, 9% from atmospheric deposition, and 1-2% from mariculture and submarine fresh groundwater discharge during this period. In the Arabian Sea (32), the total external N inputs increased from 1754 Gg/yr in 2000 to 3168 Gg/yr in 2015, with an average proportion of 48% from river export, 51% from atmospheric deposition, and 1% from mariculture and submarine fresh groundwater discharge during this period. The South China Sea (36) showed an increase of 1390 Gg/yr in its total external N inputs during the aforementioned period, with an average contribution of 65% from river export, 31% from atmospheric deposition, and 4% from mariculture and submarine fresh groundwater discharge. The Benguela Current (29) increased by about 2 times, with river export accounting for an average of 74% of total N inputs in this period and the rest 26% from atmospheric deposition.

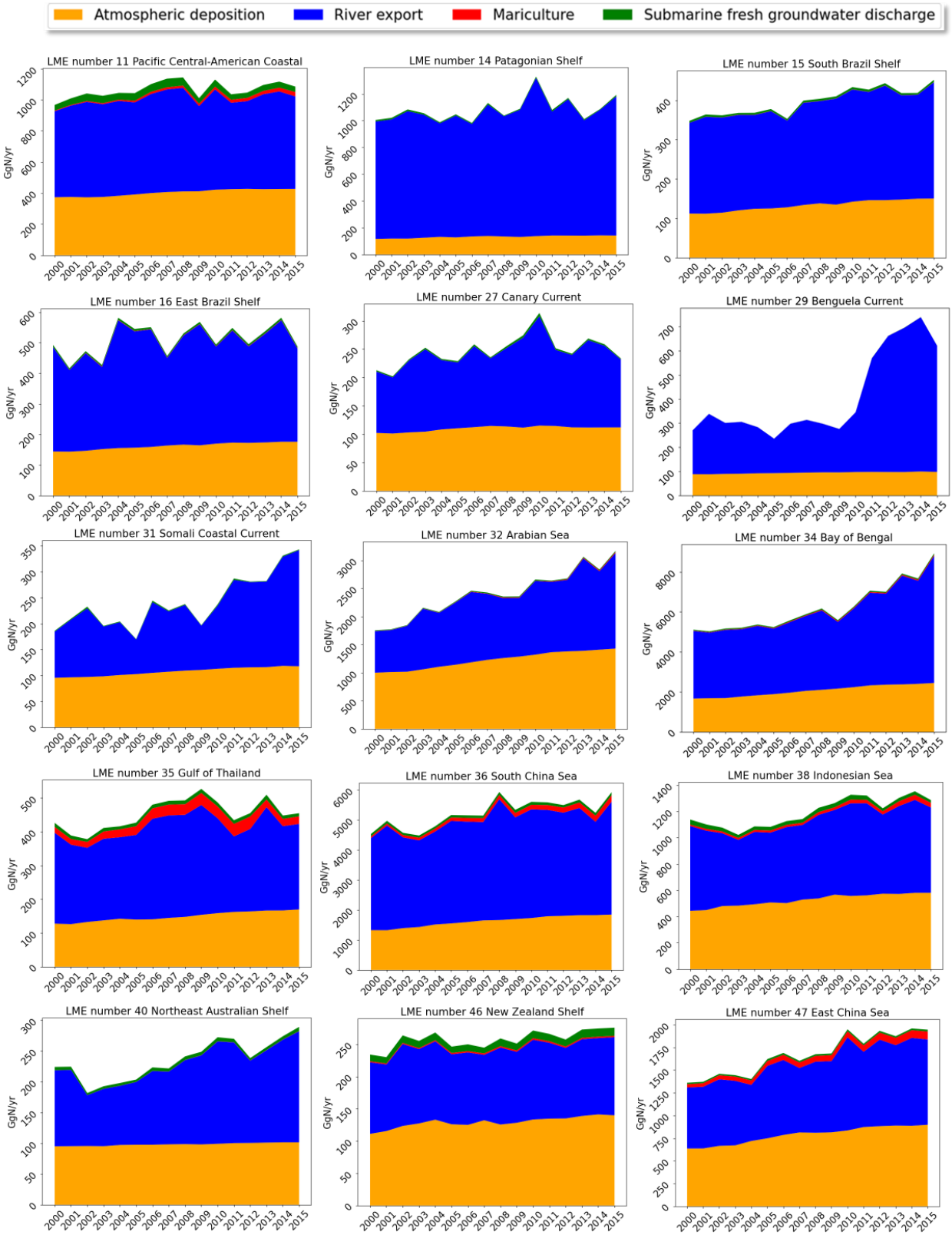

(To be continued on page 12)

(following plots on page 11)

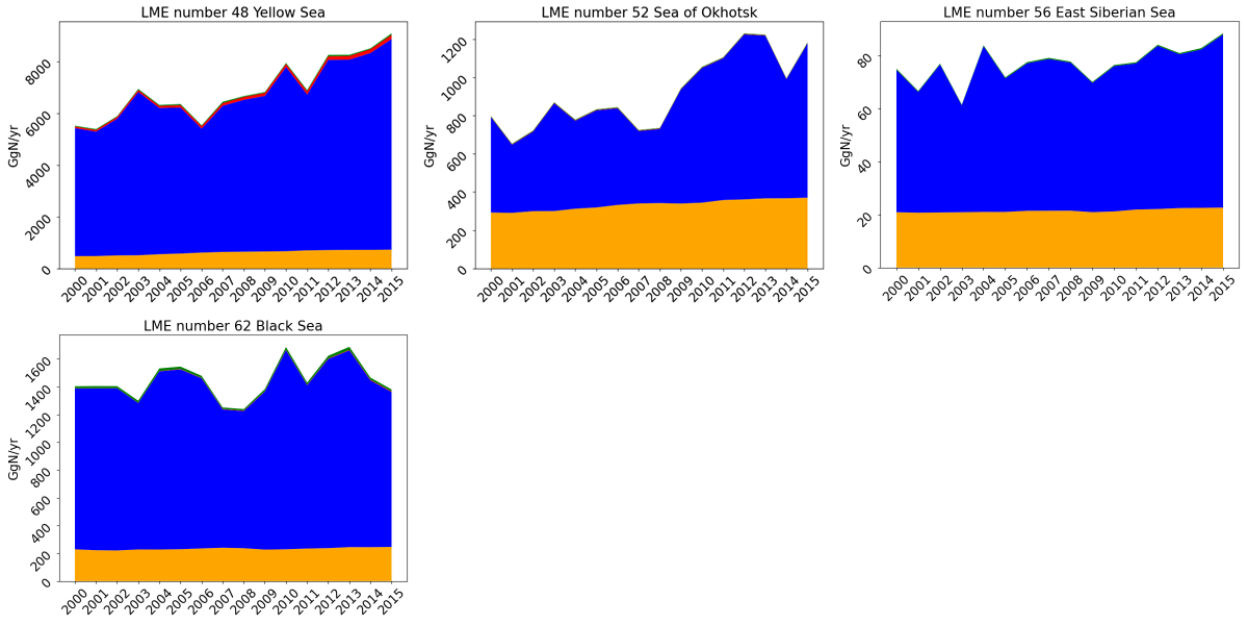

Figure 3. Long-term changes in total nitrogen inputs from 2000 to 2015 for LMEs with an overall increasing trend and a dominance by river export in total nitrogen inputs.

Fourteen LMEs showed an increasing trend of the total external N inputs with dominance by atmospheric deposition (Figure 4). For example, in the Guinea Current (28), the total N inputs increased from 1152 Gg/yr in 2000 to 1437 Gg/yr in 2015, with an average contribution of 59% from atmospheric deposition, 40% from river export, and 1% from mariculture and submarine fresh groundwater discharge. The Kuroshio Current (49) saw a 117 Gg/yr increase in total N inputs during this period, with an average share of 61% from atmospheric deposition, 35% from river export, 3% from submarine fresh groundwater discharge, and 1% from mariculture over this period. Similarly, the total N inputs in the West Bering Sea (53) increased from 368 Gg/yr in 2000 to 467 Gg/yr in 2015, with an average proportion of 55% from atmospheric deposition, 41% from river export, and 4% from submarine fresh groundwater discharge during this period.

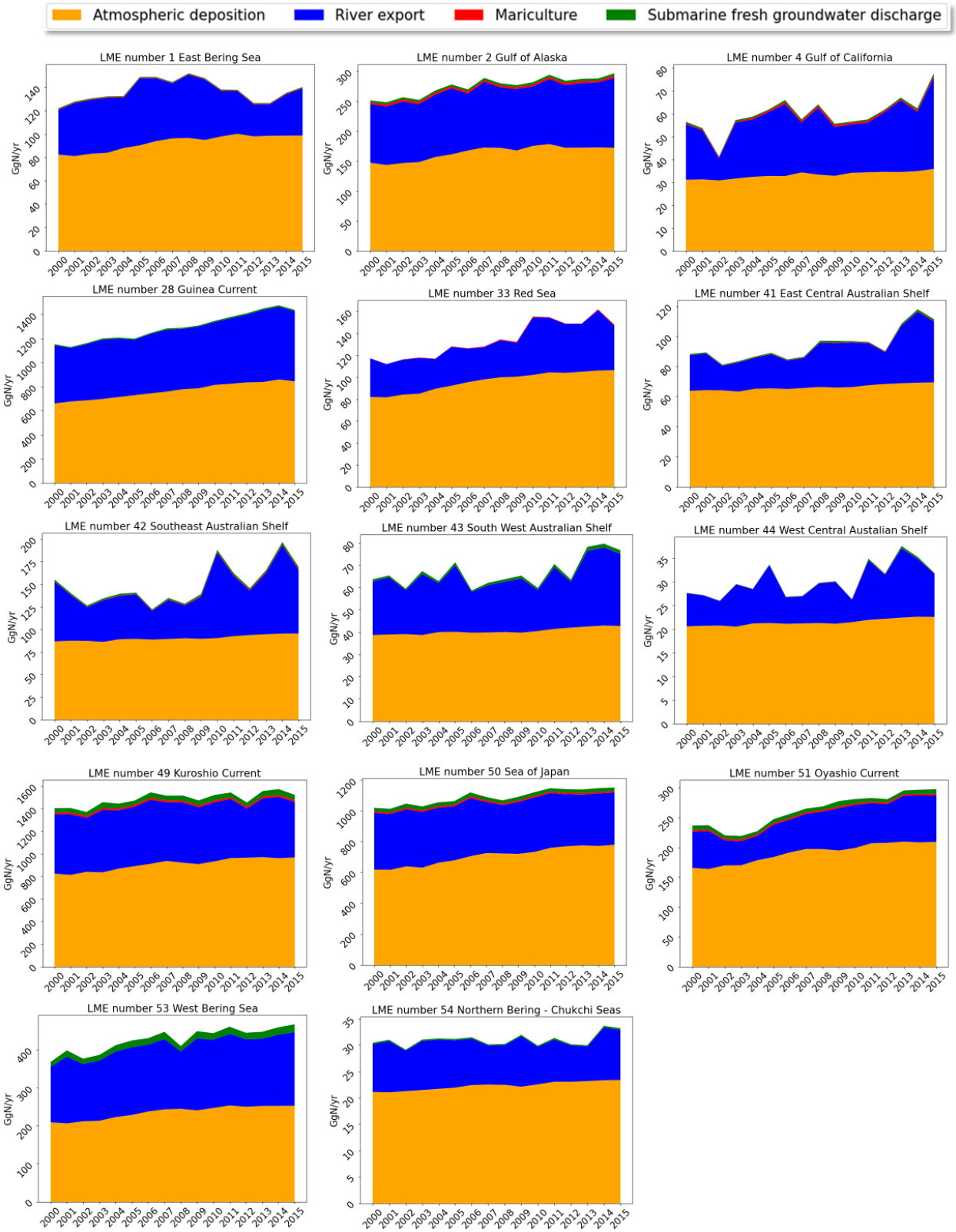

Figure 4. Long-term changes in total nitrogen inputs from 2000 to 2015 for LMEs with an overall increasing trend and dominance by atmospheric deposition in total nitrogen inputs.

4.1.2 LMEs with stabilized total external N inputs during 2000-2015

Twenty-one LMEs experienced a stable trend from all four sources during 2000-2015 (Figures 5-6). These LMEs are the California Current (3), the Northeast U.S. Continental Shelf (7), the Scotian Shelf (8), the Newfoundland-Labrador Shelf (9), the Insular Pacific-Hawaiian (10), the Caribbean Sea (12), the East Greenland Shelf (19), the Barents Sea (20), the Norwegian Sea (21), the Baltic Sea (23), the Mediterranean Sea (26), the Agulhas Current (30), the Sulu-Celebes Sea (37), the Indonesian Sea (38), the North Australian Shelf (39), the Northwest Australian Shelf (45), the Laptev Sea (57), the Kara Sea (58), the Faroe Plateau (60), the Hudson Bay Complex (63), the Aleutian Islands (65), and the Canadian High Arctic - North Greenland (66).

Twelve of the aforementioned LMEs demonstrated a dominance of river export in their total external N inputs from 2000 to 2015 (Figure 5). For example, the Northeast U.S. Continental Shelf (7) received an average of 649 Gg/yr of total N inputs during 2000-2015, In this LME the river export accounted for an average share of 75%, and atmospheric deposition accounted for an average share of 25%. The Northwest Australian Shelf (45) received an average of 162 Gg/yr of total N inputs during 2000-2015, with an average contribution of 49% from river export, 46 % from atmospheric deposition, 3% from mariculture, and 2% from submarine fresh groundwater discharge. The Aleutian Islands (65) received an average of 86 Gg/yr of total N inputs from 2000 to 2015 with an average proportion of 68% from river export, 29% from atmospheric deposition, and 3% from submarine fresh groundwater discharge.

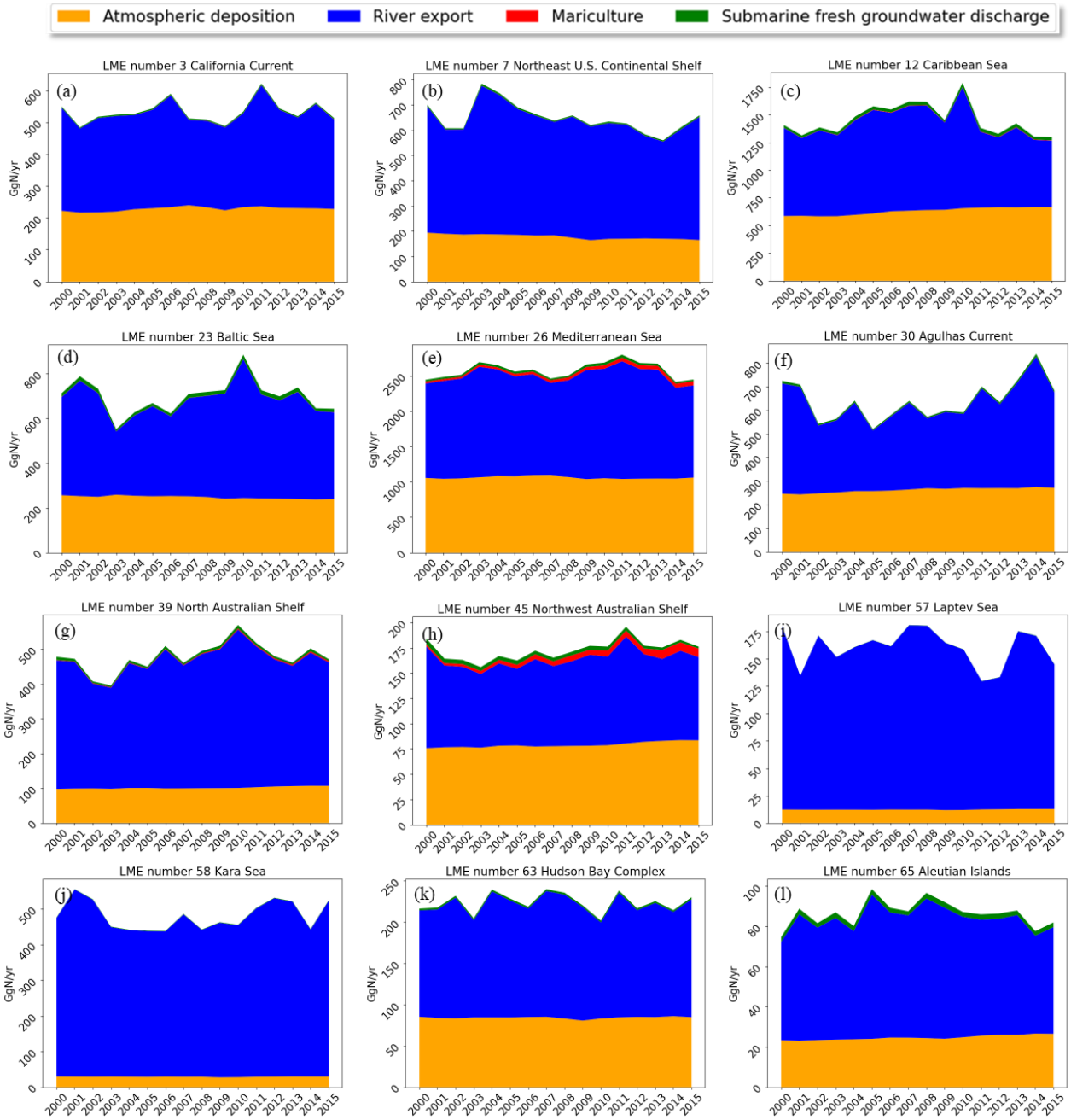

Figure 5. Long-term changes in total nitrogen inputs from 2000 to 2015 for LMEs with an overall stable trend and dominance by river export in total nitrogen inputs.

Nine LMEs with stable total external N inputs during 2000-2015 received a dominant contribution from atmospheric deposition (Figure 6). For instance, the Norwegian Sea (21) received an average of 160 Gg/yr of total N inputs during the aforementioned period, with an average contribution of 69% from atmospheric deposition, 17% from river export, 13% from mariculture, and 1% from submarine fresh groundwater discharge. The Faroe Plateau (60) received an average of 23 Gg/yr of total N inputs during this period, with an average proportion of 84% from atmospheric deposition, 10% from mariculture, and 6% from river export.

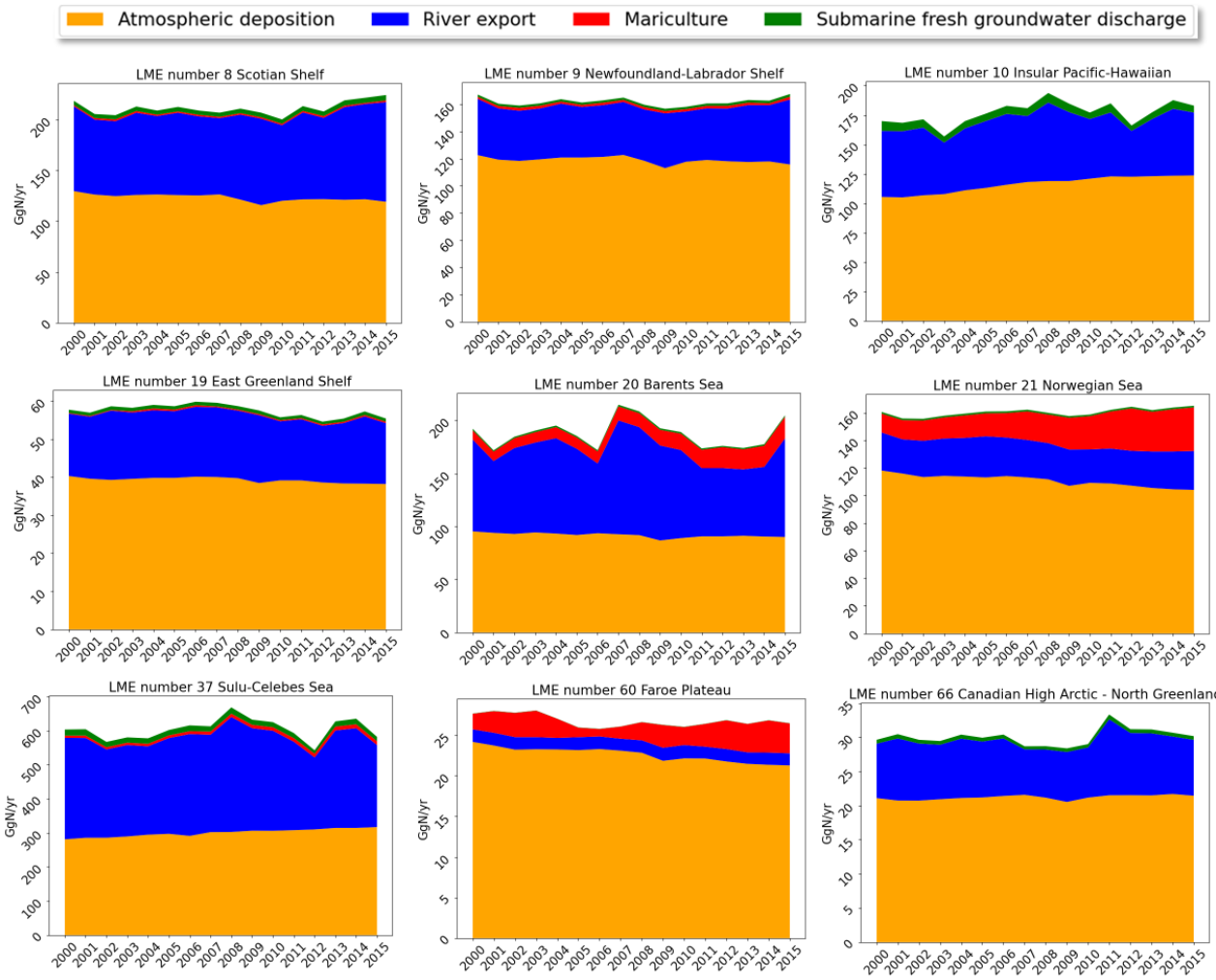

Figure 6. Long-term changes in total nitrogen inputs from 2000 to 2015 for LMEs with an overall stable trend and dominance by atmospheric deposition in total nitrogen inputs.

4.1.3 LMEs with decreasing trends in total external N inputs during 2000-2015

Eight LMEs showed a decreasing trend in their total external N inputs from all four sources during 2000-2015 (Figures 7-8). These LMEs are the Gulf of Mexico (5), the Southeast U.S. Continental Shelf (6), the Humboldt Current (13), the North Brazil Shelf (17), the North Sea (22), the Celtic-Biscay Shelf (24), the Iberian Coastal (25), and the Beaufort Sea (55).

Among these LMEs showing decreases in their external N inputs from 2000 to 2015, river export dominated the total N inputs in seven LMEs (Figure 7). For example, the Gulf of Mexico (5) experienced a decrease of 1287 Gg/yr N during the aforementioned period, with an average contribution of 77% from river export, 22% from atmospheric deposition, and 1% from mariculture and submarine fresh groundwater discharge. The total N inputs in Humboldt Current (13) decreased from 501 Gg/yr in 2000 to 449 Gg/yr in 2015, with an average share of 66% from river export, 26% from atmospheric deposition, 7% from mariculture, and 1% from submarine fresh groundwater discharge.

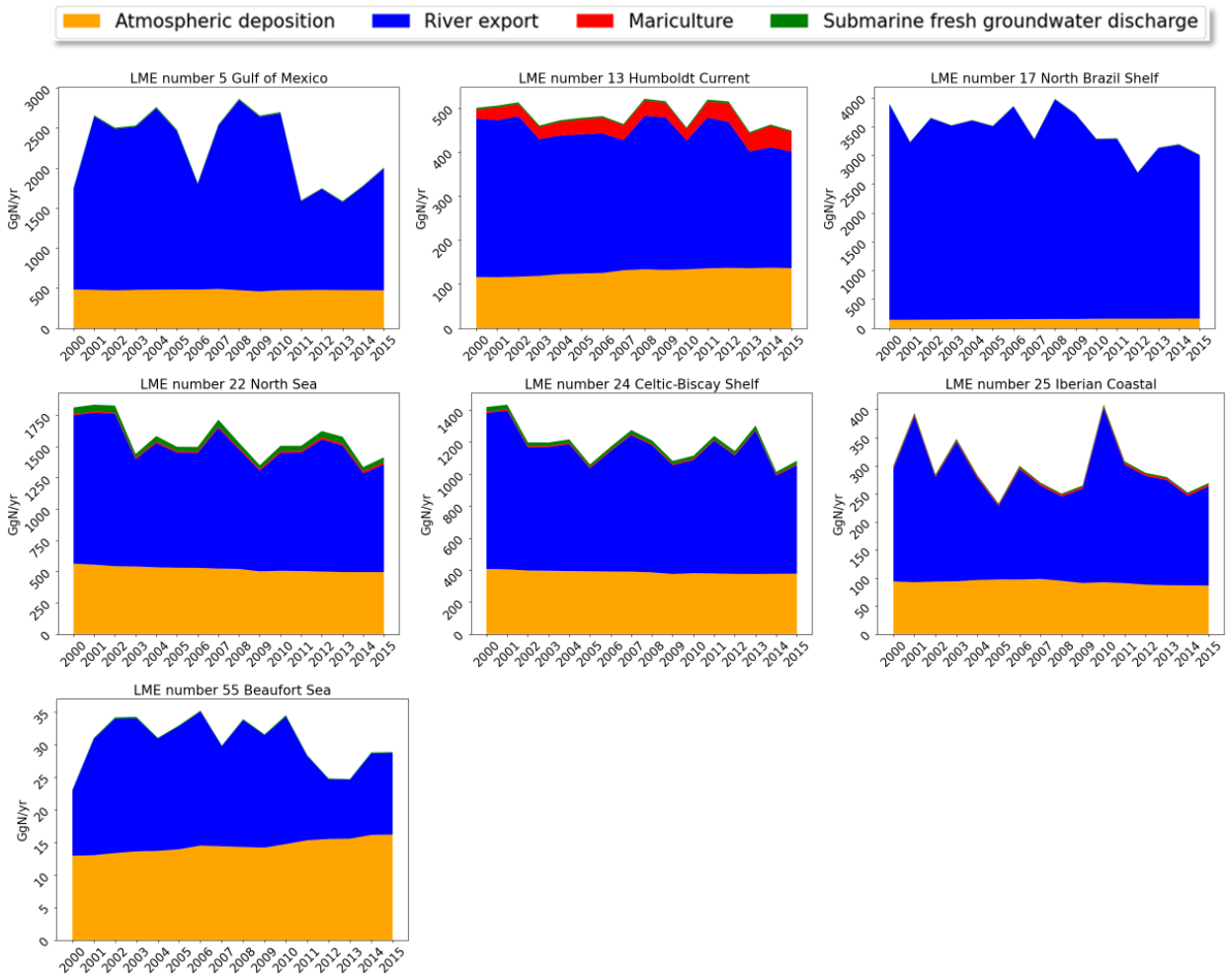

Figure 7. Long-term changes in total nitrogen inputs from 2000 to 2015 for LMEs with an overall decreasing trend and dominance by river export in total nitrogen inputs.

Only one LME showed a decrease in total N inputs from 2000-2015 with a dominance by atmospheric deposition (Figure 8). For example, the Southeast U.S. Continental Shelf (6) witnessed a decrease of 34 Gg/yr in total N inputs during the aforementioned period, with an average contribution of 58% from atmospheric deposition, 41% from river export, and 1% from mariculture and submarine fresh groundwater discharge.

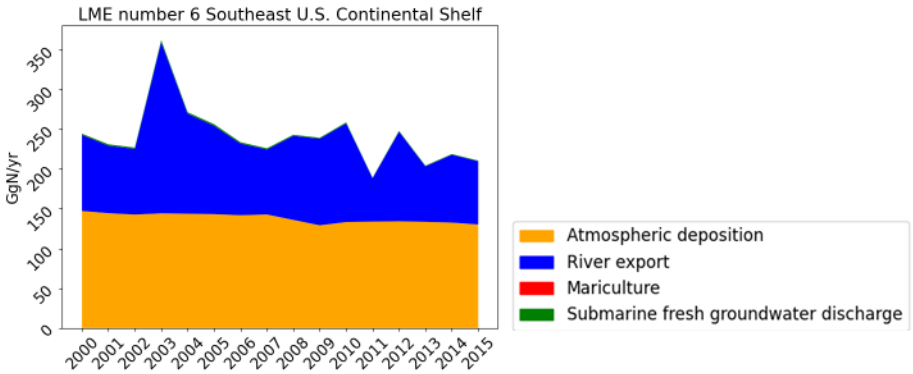

Figure 8. Long-term changes in total nitrogen inputs from 2000 to 2015 for the LME with an overall decreasing trend and dominance by atmospheric deposition.

4.1.4 Sources of river nitrogen export

River N export is influenced by a variety of factors, encompassing both natural processes and human activities, which collectively shape N dynamics within LMEs worldwide from 2000 to 2015. These factors can be classified into natural inputs, arising from geological and biological processes, and anthropogenic inputs, resulting from human activities. Understanding the relative contributions of these sources is vital for comprehending the complex mechanisms driving the changes in N export to LMEs. Natural N sources include N from natural systems via groundwater and surface runoff, and vegetation in floodplains, while anthropogenic sources comprise N from agricultural systems via groundwater and surface runoff, point sources, aquaculture, and atmospheric deposition.

4.1.4.1 LMEs with river export dominated by natural sources

In twenty-one LMEs, natural sources play a significant role as a dominant source of their received river N export (Figure 9). These LMEs are the East Bering Sea (1), the Gulf of Alaska (2), the Scotian Shelf (8), the Newfoundland-Labrador Shelf (9), the Insular Pacific-Hawaiian (10), the North Brazil Shelf (17), the East Greenland Shelf (19), the Barents Sea (20), the Norwegian Sea (21), the Benguela Current(29), the North Australian Shelf (39), the Northeast Australian Shelf (40), the Oyashio Current (51), the West Bering Sea (53), the Northern Bering - Chukchi Seas (54), the Beaufort Sea (55), the East Siberian Sea (56), the Laptev Sea (57), the Hudson Bay Complex (63), the Aleutian Islands (65), and the Canadian High Arctic - North Greenland (66).

In nine LMEs, the overall river N export with dominance by natural sources showed an increasing trend during 2000-2015. For example, the river export to the Benguela Current (29) increased by about a factor of two during this period, with an average contribution of 43% from natural systems via groundwater,17% from floodplain vegetation, and the rest from anthropogenic sources. The river export to the West Bering Sea (53) increased from 146 Gg N/yr to 210 Gg N/yr during the aforementioned period, with an average share of 38% from floodplain vegetation, 39% from groundwater under the natural lands, 7% from natural systems via surface runoff, and the rest from anthropogenic sources. The river export to the Northeast Australian Shelf (40) increased from 123 Gg N/yr in 2000 to 181 Gg N/yr in 2015, with an average proportion of 46% from floodplain vegetation, 43% from groundwater under natural lands, 5% from natural systems via surface runoff, and the rest from anthropogenic sources.

River N export to nine LMEs stayed roughly stable during 2000-2015. For example, the river export to the Aleutian Islands (65) received an average of 59 Gg N/yr during this period, with an average proportion of

65% from natural systems via groundwater, 22% from natural systems via surface runoff, 10% from floodplain vegetation, and the rest from anthropogenic sources. The North Australian Shelf (39) received an average of 367 Gg N/yr of river export during the aforementioned period, with an average contribution of 74% from floodplain vegetation, 20% from groundwater under natural lands, and the rest from anthropogenic sources. The Barents Sea (20) received about 81 Gg N/yr of river export from 2000 to 2015, and on average natural systems via groundwater accounted for 54%, vegetation on floodplains for 23%, natural systems via surface runoff for 11%, and rest is from anthropogenic sources.

Three LMEs demonstrated a decrease in their received N export from rivers during 2000-2015. As an example, the North Brazil Shelf (17) showed a decrease of 905 Gg N/yr in their river export during this period, with an average contribution of 49% from floodplain vegetation, 32% from groundwater under natural lands, 4% from surface runoff on natural lands, and the rest from anthropogenic sources.

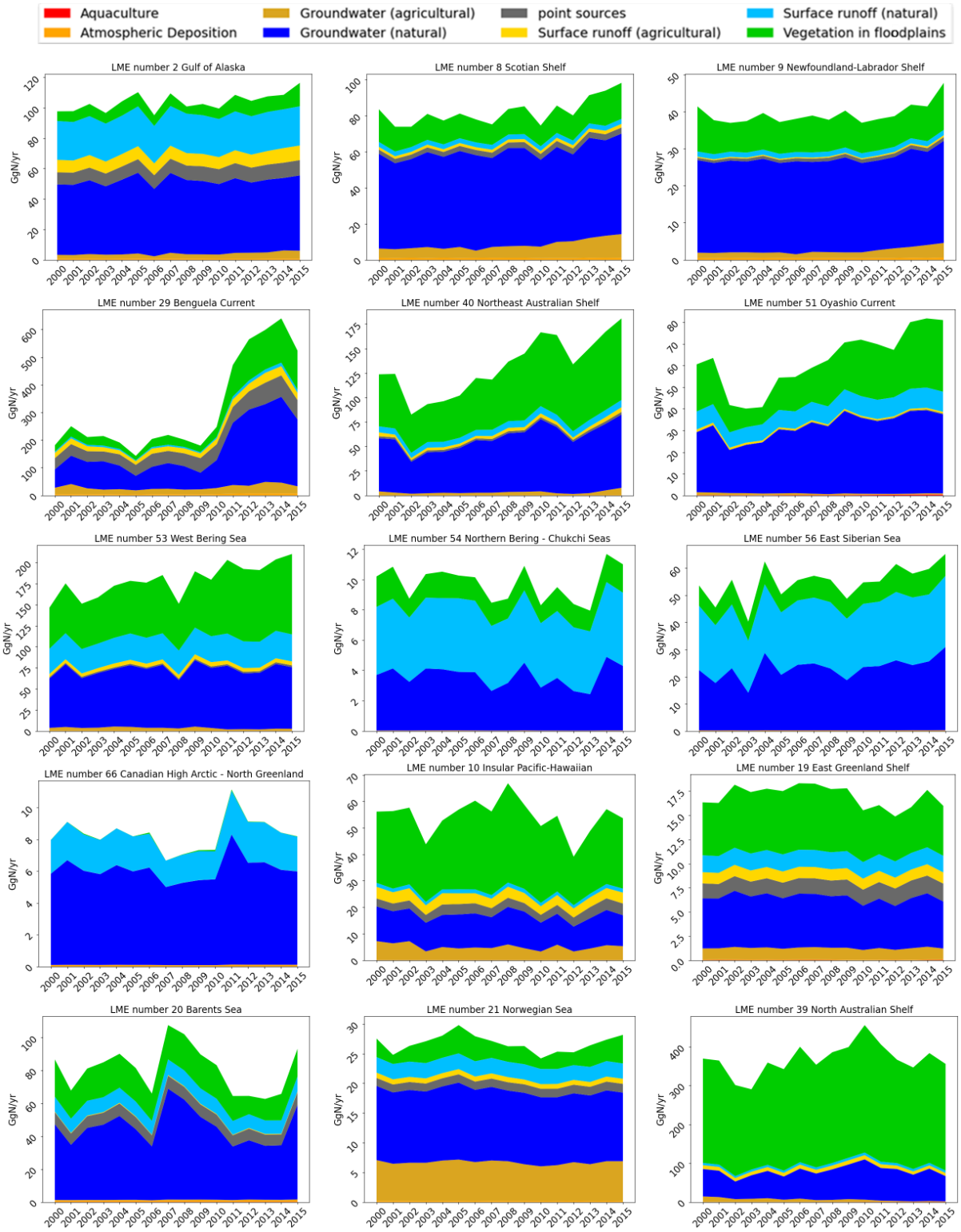

(To be continued on page 21)

(Following plots on page 20)

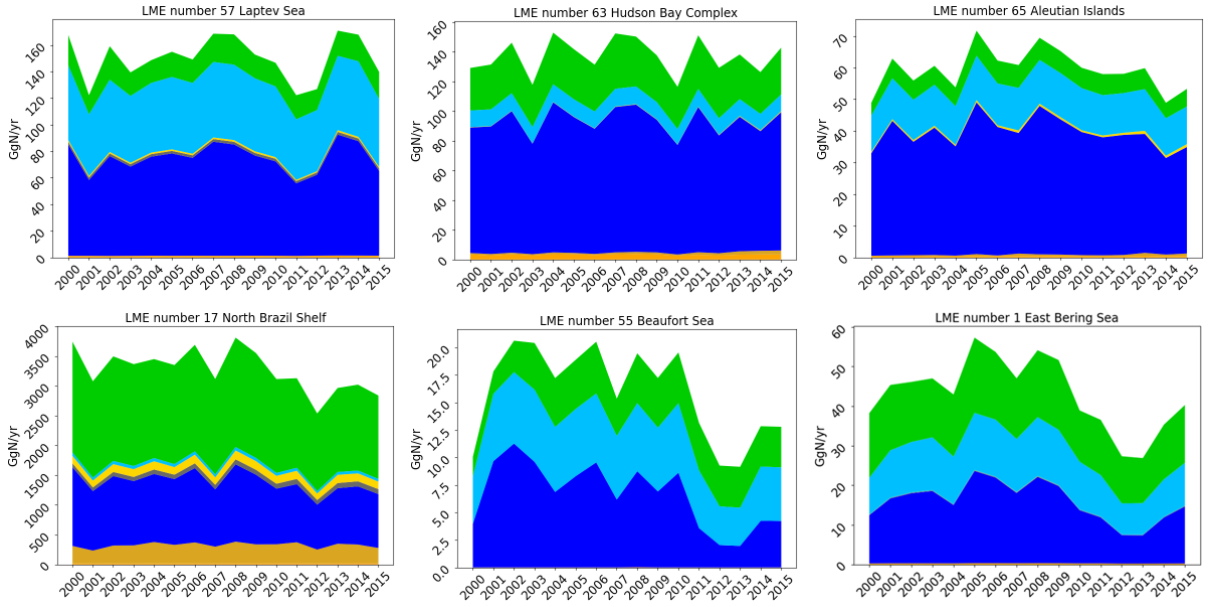

Figure 9. Long-term changes in river nitrogen export from 2000 to 2015 for LMEs with a dominance of natural sources in their river export.

4.1.4.2 LMEs with river export dominated by anthropogenic sources

In contrast, in more (Thirty-two) LMEs, human activities play a significant role as a dominant source of river N export (Figure 10). These LMEs are the California Current (3), the Gulf of California (4), the Gulf of Mexico (5), the Southeast U.S. Continental Shelf (6), the Pacific Central-American Coastal (11), the Caribbean Sea (12), the Humboldt Current (13), the Patagonian Shelf (14), the South Brazil Shelf (15), the East Brazil Shelf (16), the North Sea (22), the Baltic Sea (23), the Celtic-Biscay Shelf (24), the Iberian Coastal (25), the Mediterranean Sea (26), the Canary Current (27), the Arabian Sea (32), the Red Sea (33), the Bay of Bengal (34), the South China Sea (36), the East Central Australian Shelf (41), the Southeast Australian Shelf (42), the South West Australian Shelf (43), the West Central Australian Shelf (44), the Northwest Australian Shelf (45), the New Zealand Shelf (46), the East China Sea (47), the Yellow Sea (48), the Kuroshio Current (49), the Sea of Okhotsk (52), the Faroe Plateau (60), and the Black Sea (62).

Eighteen LMEs witnessed an increasing trend in their received river N export with a dominance of anthropogenic sources during 2000-2015. In particular, the river export to Yellow Sea (48) increased from 4956 Gg N/yr in 2000 to 8148 Gg/yr in 2015, with agricultural sources via groundwater accounting for an average contribution of 45%, point sources accounting for an average contribution of 20%, agricultural sources via surface runoff accounting for an average contribution of 19%, aquaculture accounting for an average contribution of 8%, and the rest from natural sources. The river N export to the Bay of Bengal (34) increased by a factor of two during the aforementioned period, with an average share of 32% from agricultural systems via groundwater, 30% from point sources, 30% from agricultural systems via surface runoff, and the rest from natural sources. The Arabian Sea (32) saw an increasing trend of 964 Gg N/yr in its river export during this period, with an average contribution of 32% from agricultural systems via groundwater, 30% from

point sources, 30% from agricultural systems via surface runoff, and the rest from natural sources. The river N export to the Sea of Okhotsk (52) increased from 498 Gg N/yr to 807 Gg/yr, with an average proportion of 39% from agricultural systems via groundwater, 19% from agricultural systems via surface runoff, 12% from point sources, and the rest from natural sources. The East China Sea (47) experienced an increasing trend of 270 Gg N/yr in its received river export during 2000-2015, with an average contribution of 34% from agricultural systems via groundwater, 33% from point sources, 12% from agricultural systems via surface runoff, 7% from aquaculture, and the rest from natural sources.

The river N export to nine LMEs was stable during 2000-2015. For instance, the Mediterranean Sea (26) received an average of 1447 Gg N/yr of river export during this period, with a contribution of 40% from point sources, 28% from agricultural surface runoff, 20% from agricultural groundwater, and the rest from natural sources. The California Current (3), received an average of 301 Gg N/yr of river export during the aforementioned period, with an average contribution of 29 % from agricultural systems via surface runoff, 23% from point sources, 17% from agricultural systems via groundwater, and the rest from natural sources. The Northwest Australian Shelf (45) received an average of 86 Gg N/yr from river export from 2000 to 2015 with an average proportion of 29% from point sources, about 23% from agricultural surface runoff, 13 % from agricultural groundwater, 7% from aquaculture, and the rest from natural sources.

Five LMEs demonstrated a decreasing trend in their river N export from 2000 to 2015. For instance, the river N export to the North Sea (22) decreased from 1188 Gg N/yr in 2000 to 861 Gg/yr in 2015, with an average contribution of 42% from agricultural systems via groundwater, 23% from point sources, 14% from agricultural systems via surface runoff, and the rest from natural sources.

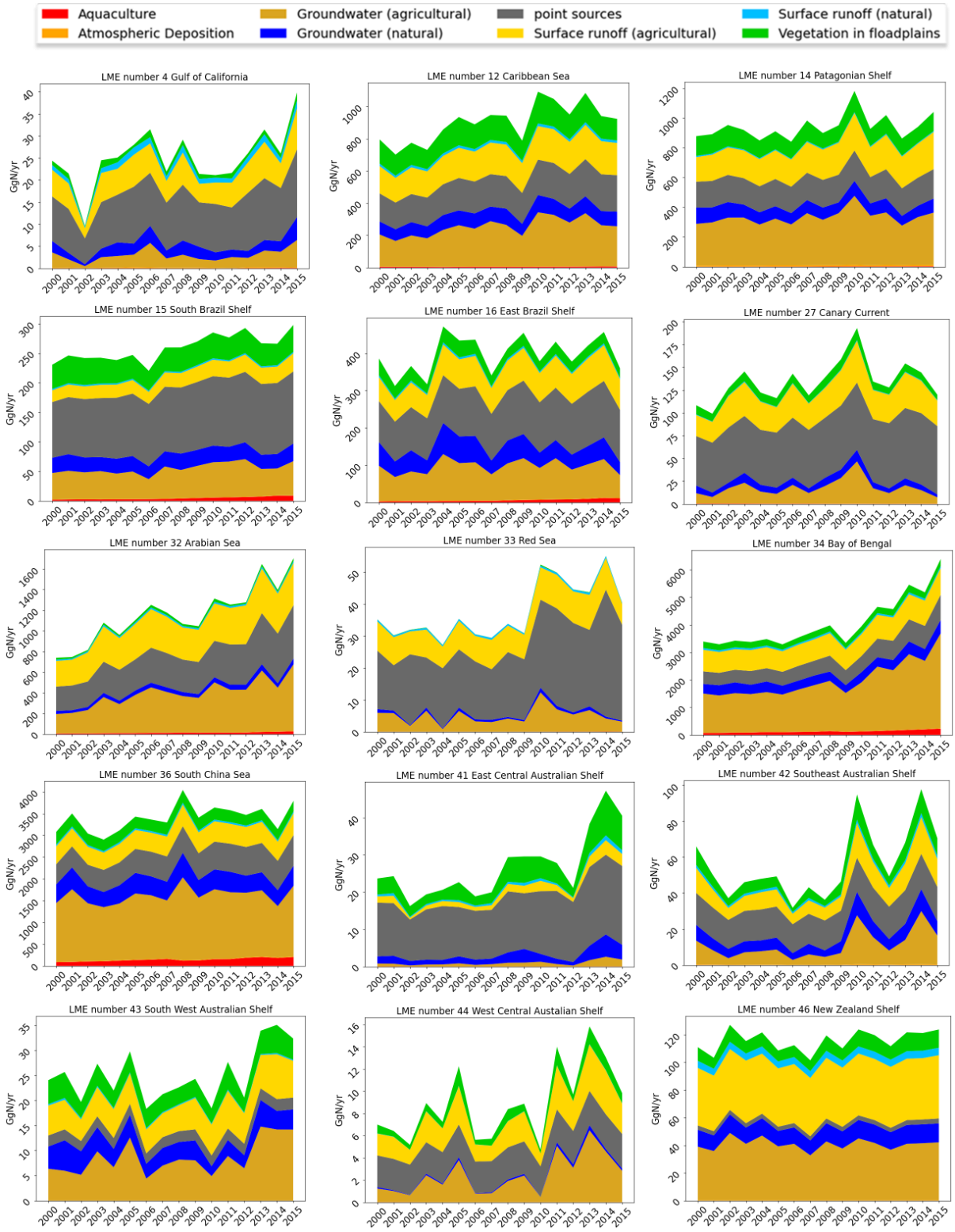

(To be continued on page 24)

(Following plots on page 23)

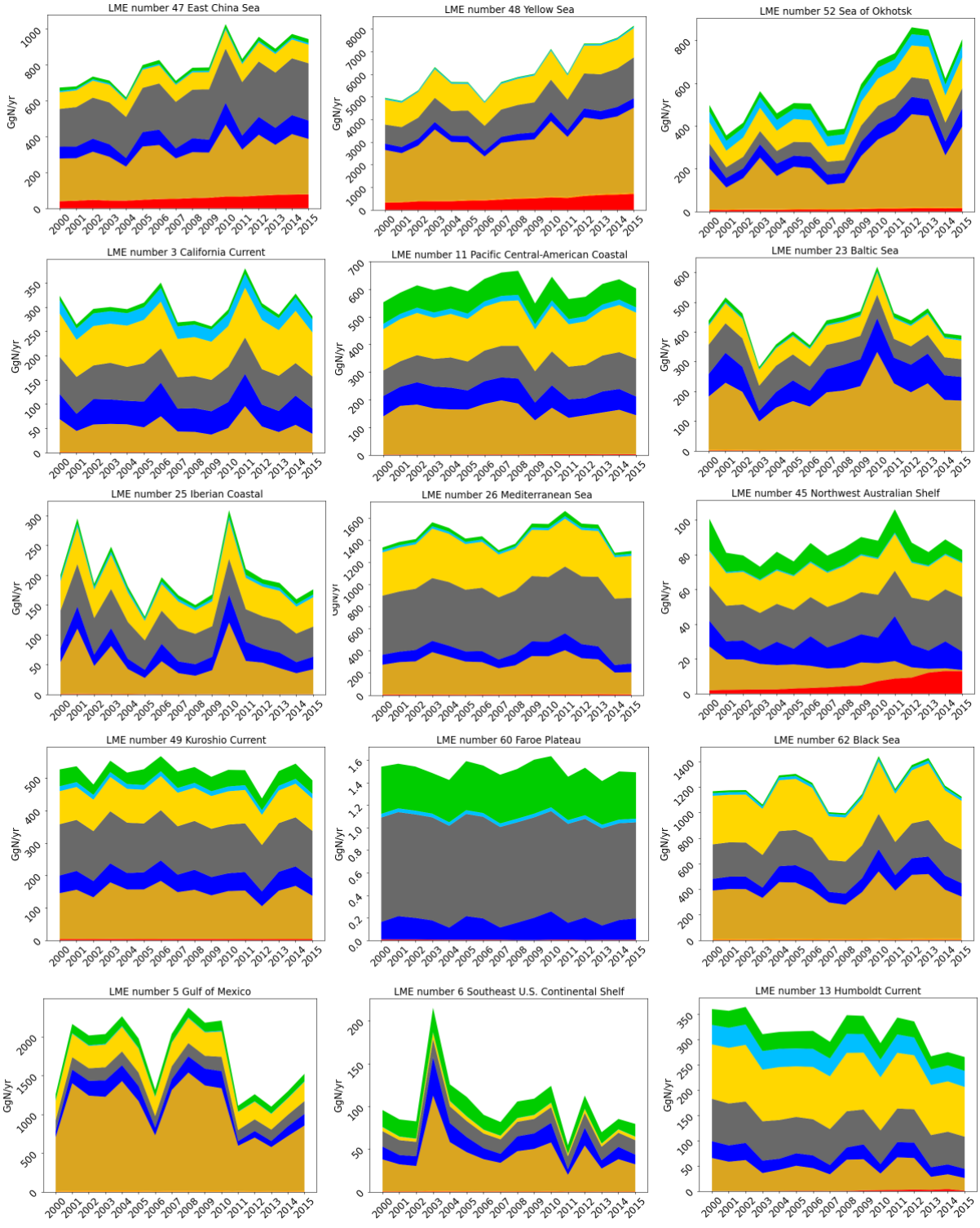

(To be continued on page 25)

(Following plots on page 24)

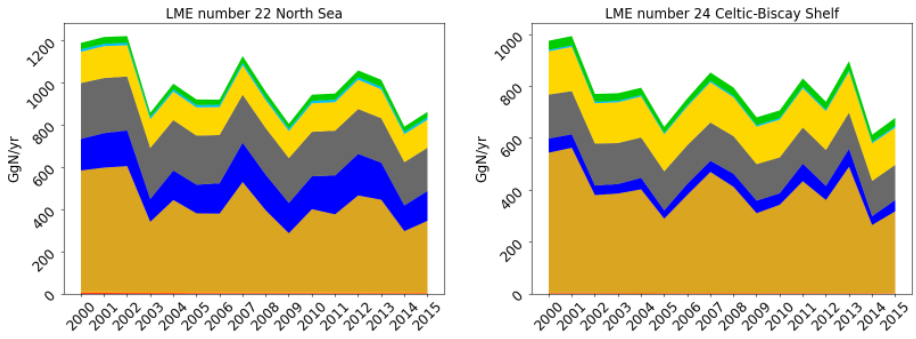

Figure 10. Long-term changes in river nitrogen export from 2000 to 2015 for LMEs with a dominance of anthropogenic sources in their river export.

4.1.4.3 LMEs with river export from similarly important anthropogenic and natural sources

In nine LMEs, both natural and anthropogenic sources are similarly important as a source of river N export (Figure 11). These LMEs are the Northeast U.S. Continental Shelf (7), the Guinea Current (28), the Agulhas Current (30), the Somali Coastal Current (31), the Gulf of Thailand (35), the Sulu-Celebes Sea (37), the Indonesian Sea (38), the Sea of Japan (50), and the Kara Sea (58).

Four LMEs showed an increasing trend in their river N export during 2000-2015. For instance, in the Somali Coastal Current (31), the N river export increased by a factor of two during this period, with an average proportion of 65% from all natural sources and 35% from all anthropogenic sources. The Indonesian Sea (38), experienced an increase of 14 Gg N/yr in its received river export during the aforementioned period, with an average contribution of 50% from natural sources and 50% from anthropogenic sources.

Four LMEs demonstrated an almost stable trend in their N input from river export during 2000-2015. For instance, the Gulf of Thailand (35) received an average of 265 Gg N/yr from river export during the aforementioned period, with an average contribution of 40% from natural sources and 60% from anthropogenic sources.

One LME, the Sea of Japan (50), showed a decreasing trend of N input from river export from 367 Gg N/yr in 2000 to 339 Gg/yr in 2015, with an average contribution of 35% from natural sources and 65% from anthropogenic sources.

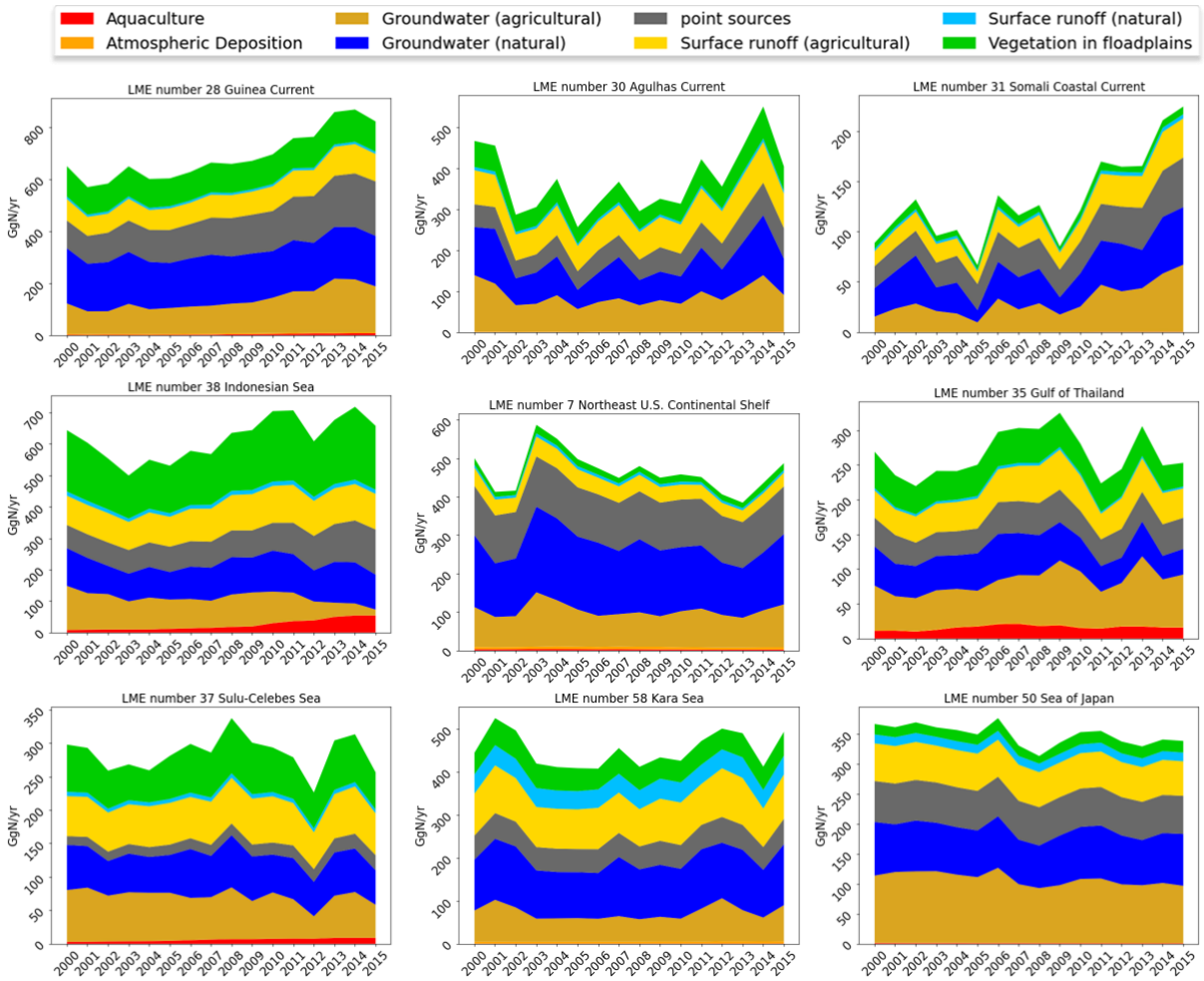

Figure 11. Long-term changes in river nitrogen export from 2000 to 2015 for LMEs with a dominance of both natural and anthropogenic sources in their river export.

4.2 Phosphorus Input

The TP tinputs increased in 32 LMEs, stayed stable in 17 LMEs, and decreased only in 13 LMEs (Figures 12-18). Similar to the N source composition, for most LMEs, river export, and atmospheric deposition play significant roles as sources of P inputs, totally accounting for 62-100% during 2000-2015 across all LMEs. The contribution of mariculture is minor for most LMEs, except for the LMEs of the Barents Sea (20), the Norwegian Sea (21), the Faroe Plateau (60), the Gulf of Thailand (35), the Northwest Australian Shelf (45), the Guinea Current (28), the Scotian Shelf(8), the South China Sea (36), the Indonesian Sea (38), the East China Sea (47), the Newfoundland-Labrador Shelf (9), the Sea of Japan (50), the Humboldt Current (13), the North Sea (22), the Sulu-Celebes Sea (37), the Kuroshio Current (49), than in other LMEs.

4.2.1 LMEs with increasing trends in total external P inputs during 2000-2015

Thirty-two LMEs showed increasing total external P inputs from all three sources during 2000-2015, with the largest contributions from rivers and atmospheric deposition (Figures 12-14). These LMEs are the Gulf of Alaska (2), the Gulf of California (4), the Scotian Shelf (8), the Patagonian Shelf (14), the South Brazil Shelf (15), the East Brazil Shelf (16), the Barents Sea (20), the Norwegian Sea (21), the Canary Current (27), the Guinea Current (28), the Benguela Current(29), the Agulhas Current (30), the Somali Coastal Current (31), the Arabian Sea (32), the Bay of Bengal (34), the South China Sea (36), the Indonesian Sea (38), the North Australian Shelf (39), the Northeast Australian Shelf (40), the East Central Australian Shelf (41), the Southeast Australian Shelf (42), the South West Australian Shelf (43), the West Central Australian Shelf (44), the Northwest Australian Shelf (45), the New Zealand Shelf (46), the East China Sea (47), the Yellow Sea (48), the Oyashio Current (51), the Sea of Okhotsk (52), the West Bering Sea (53), the East Siberian Sea (56), and the Faroe Plateau (60).

Twenty-three LMEs demonstrated an increasing trend in total external P inputs with a dominance of river export during 2000-2015. For example, the Bay of Bengal (34) experienced an increase of 169 Gg/yr of total P inputs during the aforementioned period, with an average contribution of 88% from river export, 11% from atmospheric deposition, and 1% from mariculture. In the South China Sea (36), there was an increase of 89 Gg/yr of total P inputs during 2000-2015, where river export accounted for 84%, atmospheric deposition accounted for 9%, and mariculture accounted for 7% on average during this period. In the Benguela Current (29), the total P inputs increased by about two times during this period, with an average share of 60% from river export and 40% from atmospheric deposition. The Indonesian Sea (38) showed an in increase in the total P inputs from 111 Gg/yr in 2000 to 127 Gg/yr in 2015, with an average contribution of 82% from river export, 16% from atmospheric deposition, and 2% from mariculture. Total P inputs in the East China Sea (47) increased by 38 Gg/yr from 2000 to 2015, with an average proportion of 71% from river export, 20% from atmospheric deposition, and 9% from mariculture.

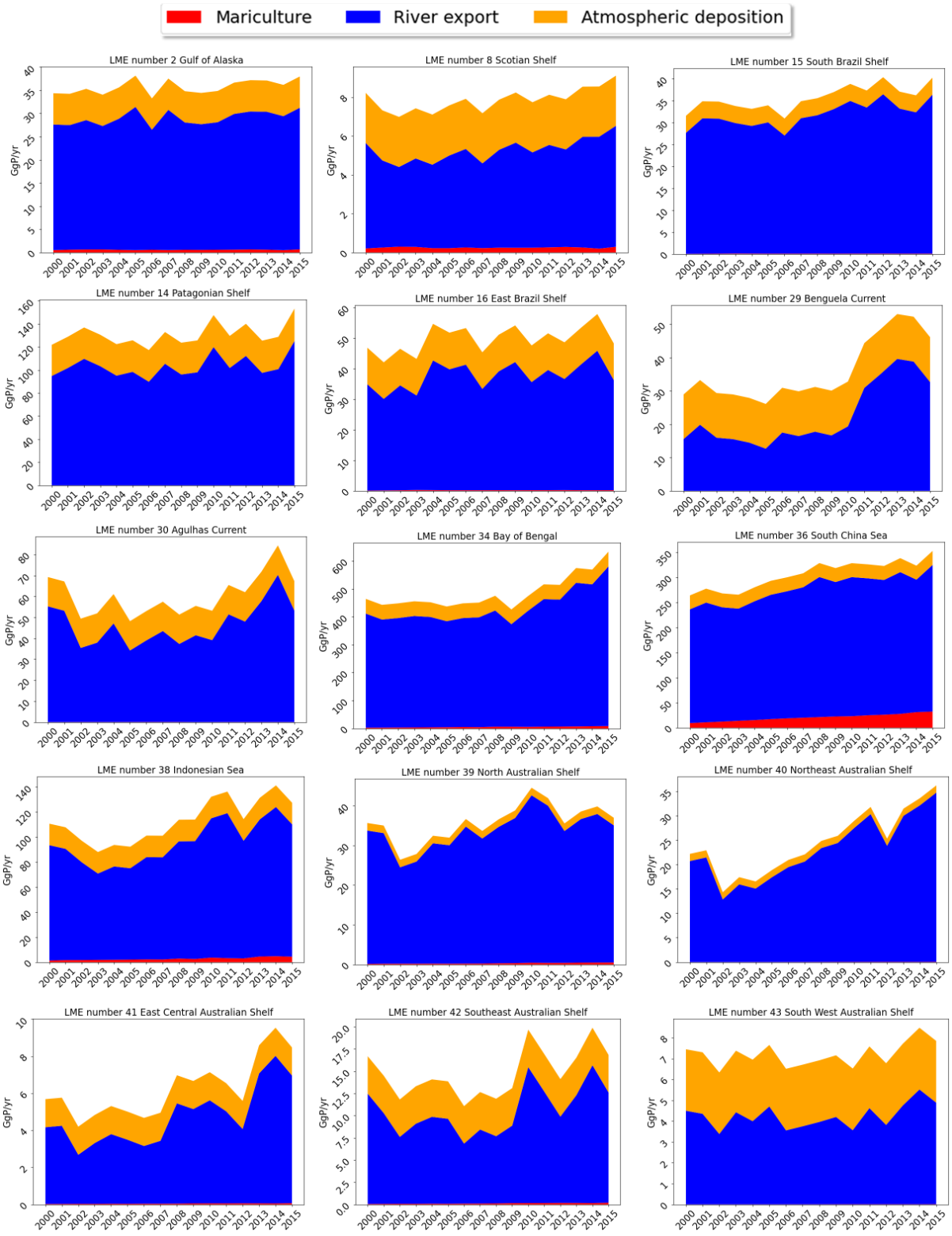

(To be continued on page 29)

(Following plots page 28)

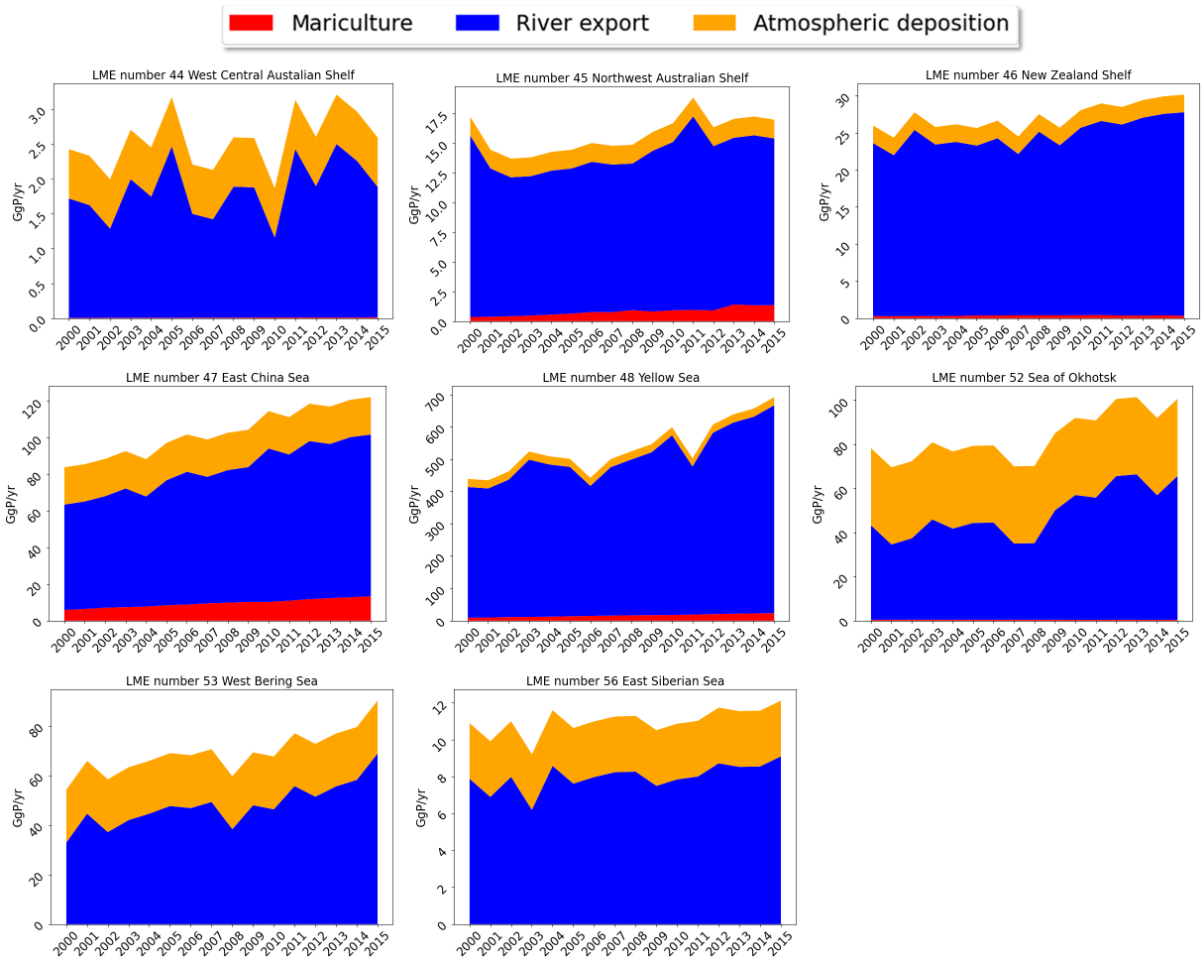

Figure 12. Long-term changes in total phosphorus inputs from 2000 to 2015 for LMEs with an overall increasing trend and dominance by river export. Twenty-three LMEs with this trend are shown.

Seven LMEs demonstrated an increasing trend in their total external P inputs with a dominance of atmospheric deposition from 2000-2015. For instance, in the Arabian Sea (32), there was an increase of 126 Gg/yr of total external P inputs from 2000 to 2015, with an average contribution of 85% from atmospheric deposition and 15% from river export. The total external P inputs to the Somali Coastal Current (31) increased from 120 Gg/yr in 2000 to 138 Gg/yr in 2015, with an average proportion of 87% from atmospheric deposition and 13% from river export. The Barents Sea (20) saw an increase of 4 Gg/yr in its total P inputs during the aforementioned period, with an average proportion of 49% from atmospheric deposition, 36% from river export, and 14% from mariculture which grew during 2000-2015.

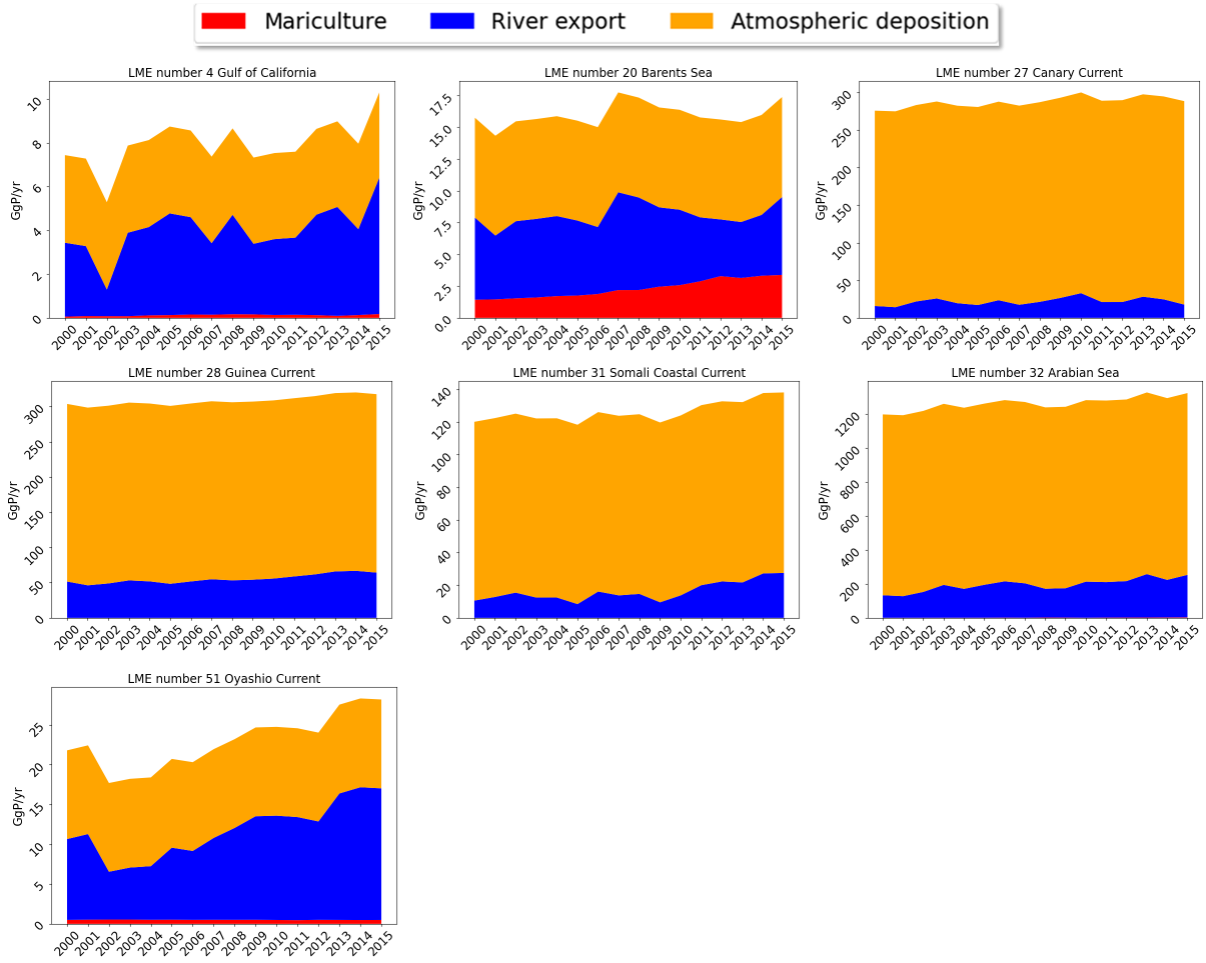

Figure 13. Long-term changes in total phosphorus inputs from 2000 to 2015 for LMEs with an overall increasing trend and dominance by atmospheric deposition. Seven LMEs with this trend are shown.

Two LMEs showed an increasing trend with a dominance of mariculture during 2000-2015. The total P inputs to the Faroe Plateau (60) increased from 0.9 Gg/yr in 2000 to 1.22 Gg/yr in 2015, with an average contribution of 39% from mariculture, 36% from atmospheric deposition, and 25% from river export. The total external P inputs to the Norwegian Sea (21) increased by 3 Gg/yr during 2000-2015, with an average contribution of 39% from atmospheric deposition, 37% from mariculture, and 23% from river export, and mariculture ranked as the largest source with a contribution of xx% in 2015.

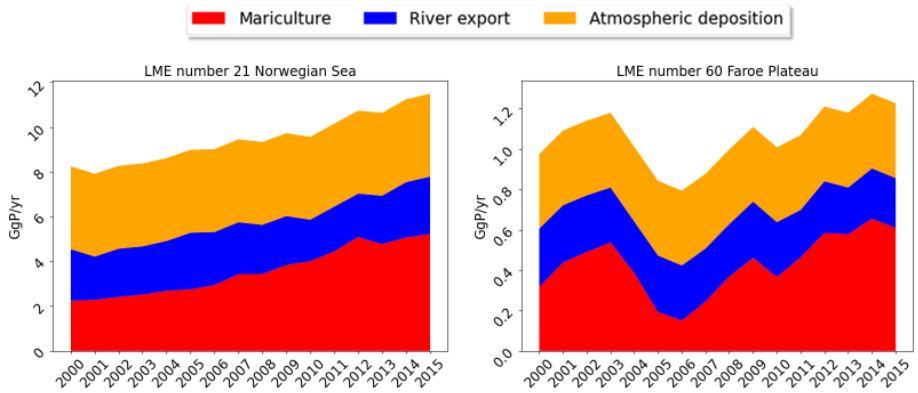

Figure 14. Long-term changes in total phosphorus inputs from 2000 to 2015 for LMEs with an overall increasing trend and dominance by mariculture. Two LMEs with this trend is shown.

4.2.2 LMEs with stabilized total external P inputs during 2000-2015

Seventeen LMEs showed an almost stable trend in their total P inputs from all three sources during 2000-2015 (Figures 15-16). These LMEs are the California Current (3), the Northeast U.S. Continental Shelf (7), the Newfoundland-Labrador Shelf (9), the Insular Pacific-Hawaiian (10), the Pacific Central-American Coastal (11), the East Greenland Shelf (19), the Mediterranean Sea (26), the Red Sea (33), the Gulf of Thailand (35), the Sea of Japan (50), the Northern Bering - Chukchi Seas (54), the Laptev Sea (57), the Kara Sea (58), the Black Sea (62), the Hudson Bay Complex (63), the Aleutian Islands (65), and the Canadian High Arctic - North Greenland (66).

Eleven LMEs received stable total external P inputs from 2000 to 2015, with dominance by river export. For example, the Pacific Central-American Coastal (11) received an average of 196 Gg/yr of total P inputs during this period, with 71% from river export, 28% from atmospheric deposition, and 1% from mariculture. The Laptev Sea (57) received an average of 34 Gg/yr of total P inputs during 2000-2015, with an average share of 93% from river export and 7% from atmospheric deposition. The Gulf of Thailand (35) received an average of 32 Gg/yr of total P inputs during the aforementioned period, with an average proportion of 68% from river export, 20% from atmospheric deposition, and 12% from mariculture.

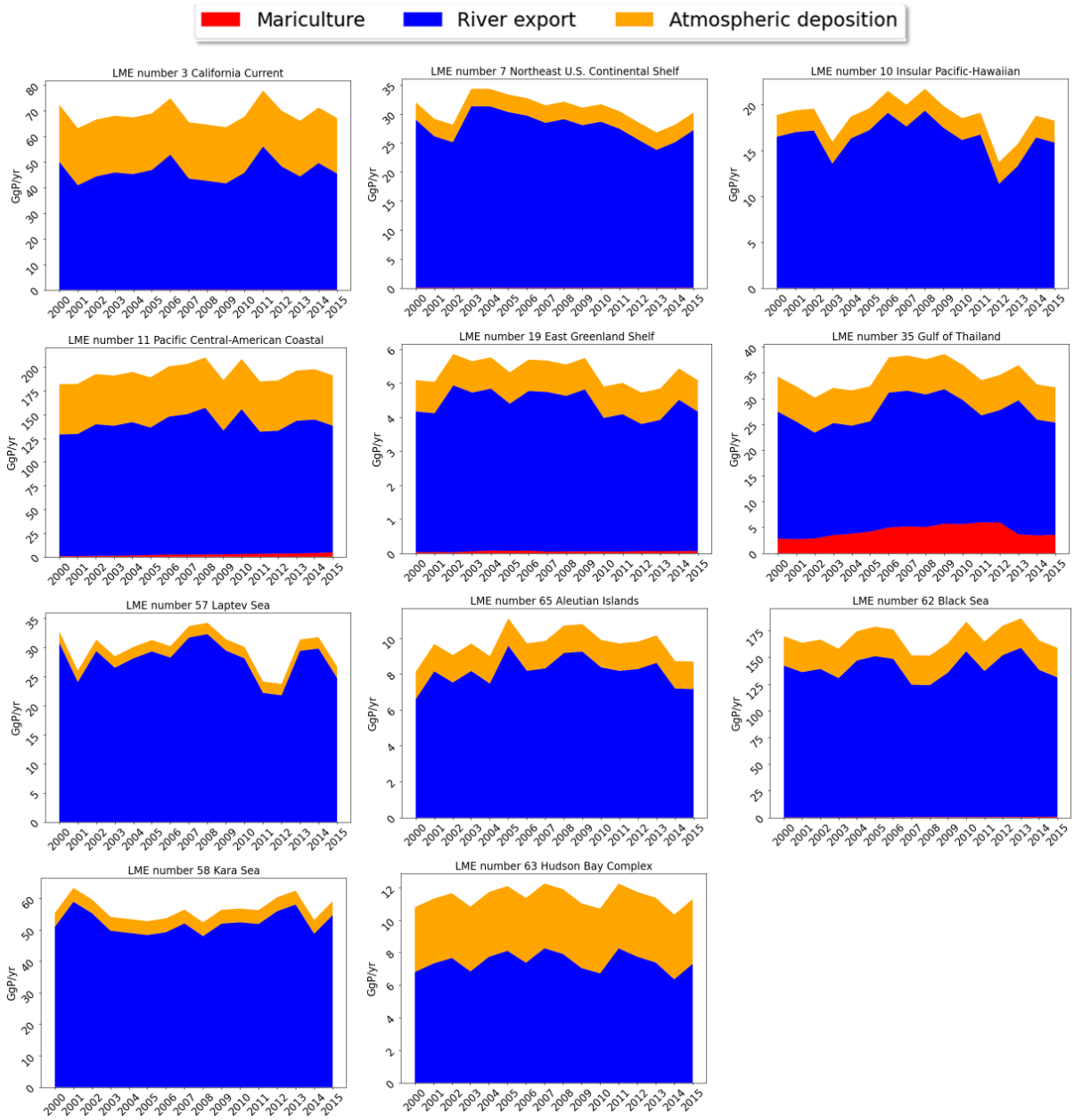

Figure 15. Long-term changes in total phosphorus inputs from 2000 to 2015 for LMEs with an overall stable trend and dominance by river export. Eleven LMEs with this trend are shown.

Six LMEs demonstrated an almost stable trend of total external P inputs during 2000-2015, with a dominance by atmospheric deposition. For example, the Red Sea (33) received an average of 392 Gg/yr of total P inputs during the aforementioned period, with an average share of 98% from atmospheric deposition and only 2% from river export. The Newfoundland-Labrador Shelf (9) received an average of 6 Gg/yr of total P inputs during this period, with an average contribution of 55% from atmospheric deposition, 40% from river export, and 5% from mariculture.

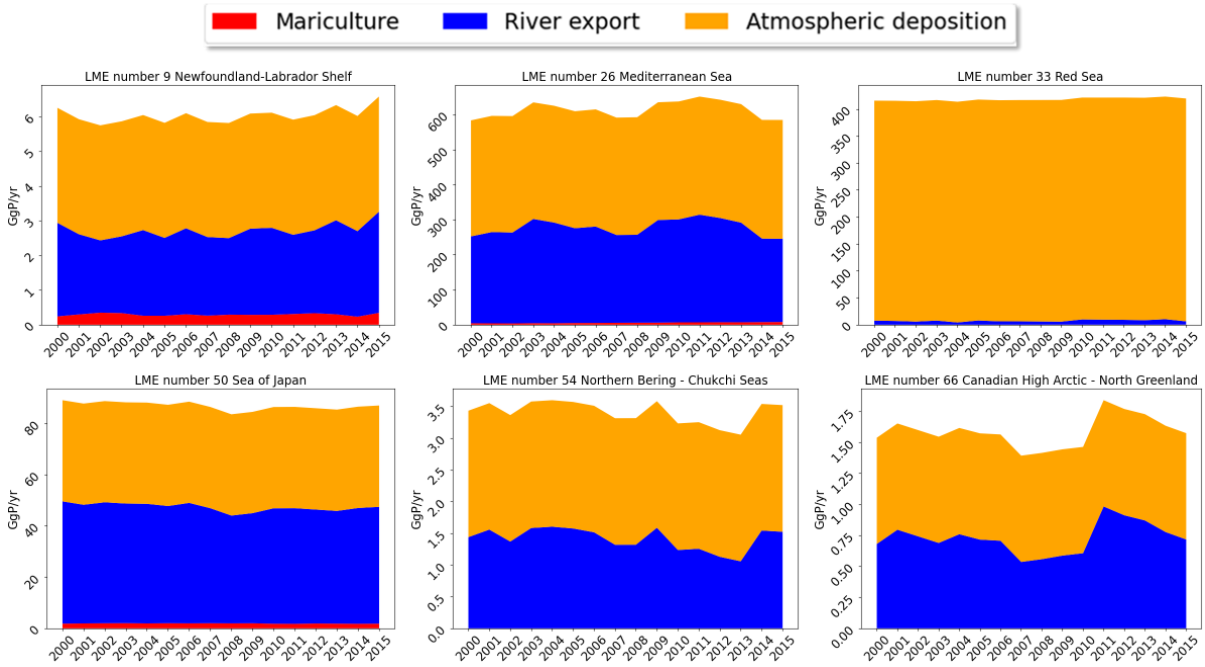

Figure 16. Long-term changes in total phosphorus inputs from 2000 to 2015 for LMEs with an overall stable trend and dominance by atmospheric deposition. Six LMEs with this trend are shown.

4.2.3 LMEs with decreasing trends in total external P inputs during 2000-2015

Thirteen LMEs showed overall decreasing trends in their total external P inputs from all three sources during 2000-2015 (Figures 17-18). These LMEs are the East Bering Sea (1), the Gulf of Mexico (5), the Southeast U.S. Continental Shelf (6), the Caribbean Sea (12), the Humboldt Current (13), the North Brazil Shelf (17), the North Sea (22), the Baltic Sea (23), the Celtic-Biscay Shelf (24), the Iberian Coastal (25), the Sulu-Celebes Sea (37), the Kuroshio Current (49), and the Beaufort Sea (55).

Eleven LMEs demonstrated a decreasing trend in total P inputs from 2000-2015, with a dominant source of river export (Figure 17). For instance, the North Brazil Shelf (17), showed a decreasing trend of 61 Gg/yr of total P inputs during this period, with an average share of 71% from river export and 29% from atmospheric deposition. Total P inputs to the Humboldt Current (13) decreased from 75 Gg/yr in 2000 to 58 Gg/yr in 2015, with an average contribution of 85% from river export, 7% from atmospheric deposition, and 8% from mariculture. The total external P inputs to the Kuroshio Current (49) decreased by 16 Gg/yr during this period, with an average proportion of 75% from river export, 24% from atmospheric deposition, and 1% from mariculture.

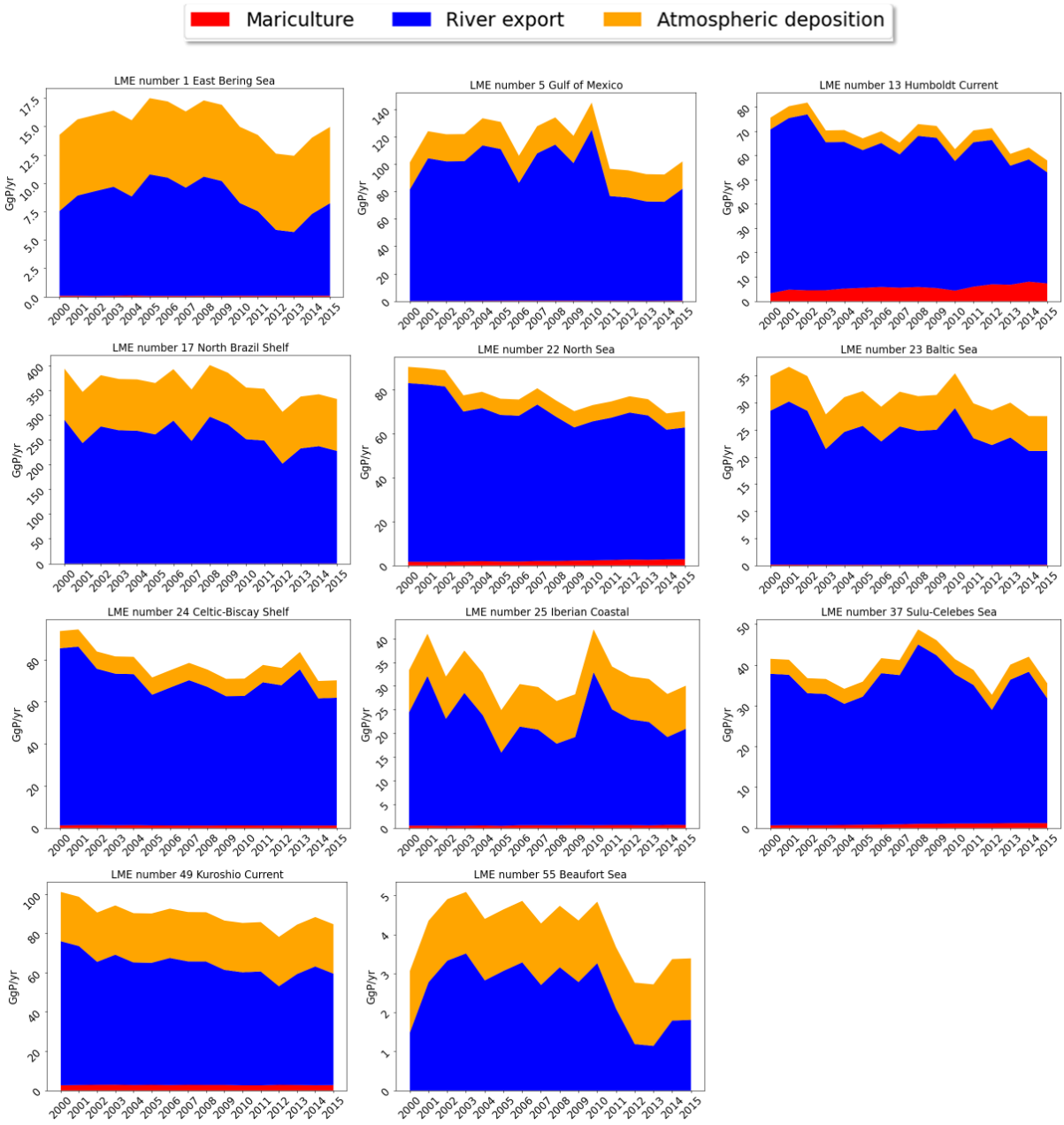

Figure 17. Long-term changes in total phosphorus inputs from 2000 to 2015 for LMEs with an overall decreasing trend and dominance by river export. Eleven LMEs with this trend are shown.

Two LMEs demonstrated a decreasing trend in total P inputs with a dominance of atmospheric deposition from 2000-2015 (Figure 18). For example, the total external P inputs to the Caribbean Sea (12) decreased by 33 Gg/yr during the aforementioned period, with an average contribution of 57% from atmospheric deposition and 43% from river export.

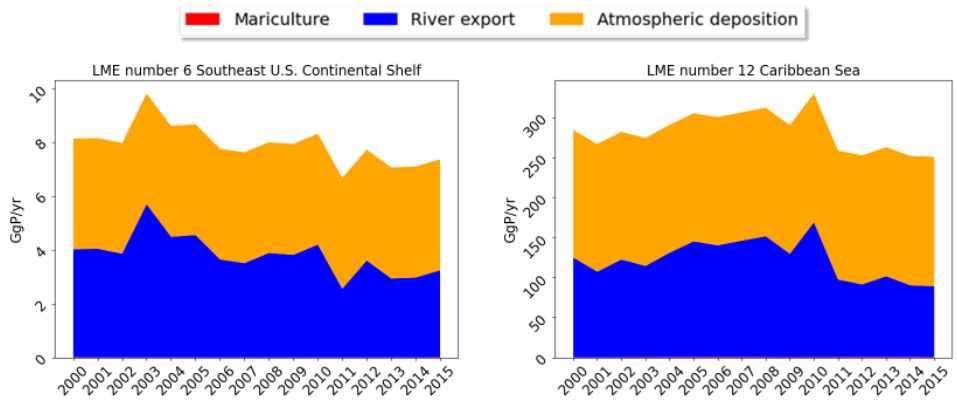

Figure 18. Long-term changes in total phosphorus inputs from 2000 to 2015 for LMEs with an overall decreasing trend and dominance by atmospheric deposition. Two LMEs with this trend are shown.

4.2.4 Sources of river phosphorus export

River P export is influenced by different factors, encompassing both natural processes and anthropogenic activities, which influence the change of total P inputs driven by river export to different LMEs from 2000 to 2015. These sources can be categorized into natural inputs arising from geological and biological processes, as well as anthropogenic inputs stemming from human activities. Natural sources include weathering, input from natural systems via surface runoff, and vegetation in floodplains, while anthropogenic sources comprise input from agricultural systems via surface runoff, point sources, and aquaculture.

4.2.4.1 LMEs with river export dominated by natural sources

In twenty LMEs, natural sources play a significant role as a dominant source of their received river P export (Figure 19). These LMEs are the East Bering Sea (1), the Gulf of Alaska (2), the Scotian Shelf (8), the Newfoundland-Labrador Shelf (9), the Insular Pacific-Hawaiian (10), the North Brazil Shelf (17), the East Greenland Shelf (19), the Barents Sea (20), the Norwegian Sea (21), the North Australian Shelf (39), the Northeast Australian Shelf (40), the Oyashio Current (51), the West Bering Sea (53), the Northern Bering - Chukchi Seas (54), the Beaufort Sea (55), the East Siberian Sea (56), the Laptev Sea (57), the Hudson Bay Complex (63), the Aleutian Islands (65), and the Canadian High Arctic - North Greenland (66).

Nine LMEs showed an increasing trend in their river P export with a dominance of natural sources from 2000 to 2015. For example, in the Oyashio Current (51), the river P export increased by about two times during this period, with an average proportion of 72% from weathering, 13% from floodplain vegetation, 12% from natural groundwater, and the rest from anthropogenic sources. In the North Australian Shelf (39), there was an increase of 4 Gg P/yr in river export during this period, with an average contribution of 55% from floodplain vegetation, 33% from weathering, 3% from natural groundwater, and the rest from anthropogenic sources. The East Siberian Sea (56) saw an increase in river P export from 8 Gg P/yr in 2000 to 9 Gg/yr in 2015, with an average contribution of 90% from natural surface runoff, 7% from floodplain vegetation, 2% from weathering, and the rest from anthropogenic sources.

Five LMEs demonstrated an almost stable trend in their river P export from 2000 to 2015, with a dominance of natural sources. For example, the Hudson Bay Complex (63) received an average of 7 Gg P/yr in river export during the aforementioned period, with an average share of 36% from weathering, 33% from floodplain vegetation, and 29% from natural systems via surface runoff. The East Greenland Shelf (19) received an

average of 4 Gg P/yr in river export from 2000 to 2015, with an average contribution of 55% from weathering, 16% from natural systems via surface runoff, and 11% from floodplain vegetation. The Norwegian Sea (21) received an average of 2 Gg P/yr in river export during this period, with an average contribution of 42% from weathering, 26% from natural surface runoff, 11% from floodplain vegetation, and the rest from anthropogenic sources.

Six LMEs showed a decreasing trend in their received river P export, with a dominance of natural sources during 2000-2015. For example, the North Brazil Shelf (17) demonstrated a decrease of 62 Gg P/yr in its river export during this period, with an average contribution of 44% from floodplain vegetation, 33% from weathering, and 4% from natural systems via surface runoff, and the rest from anthropogenic sources. The river P export to the East Bering Sea (1) increased by 1 Gg P/yr during the aforementioned period, with an average share of 75% from natural systems via surface runoff, 13% from floodplain vegetation, 11% from weathering, and the rest from anthropogenic sources.

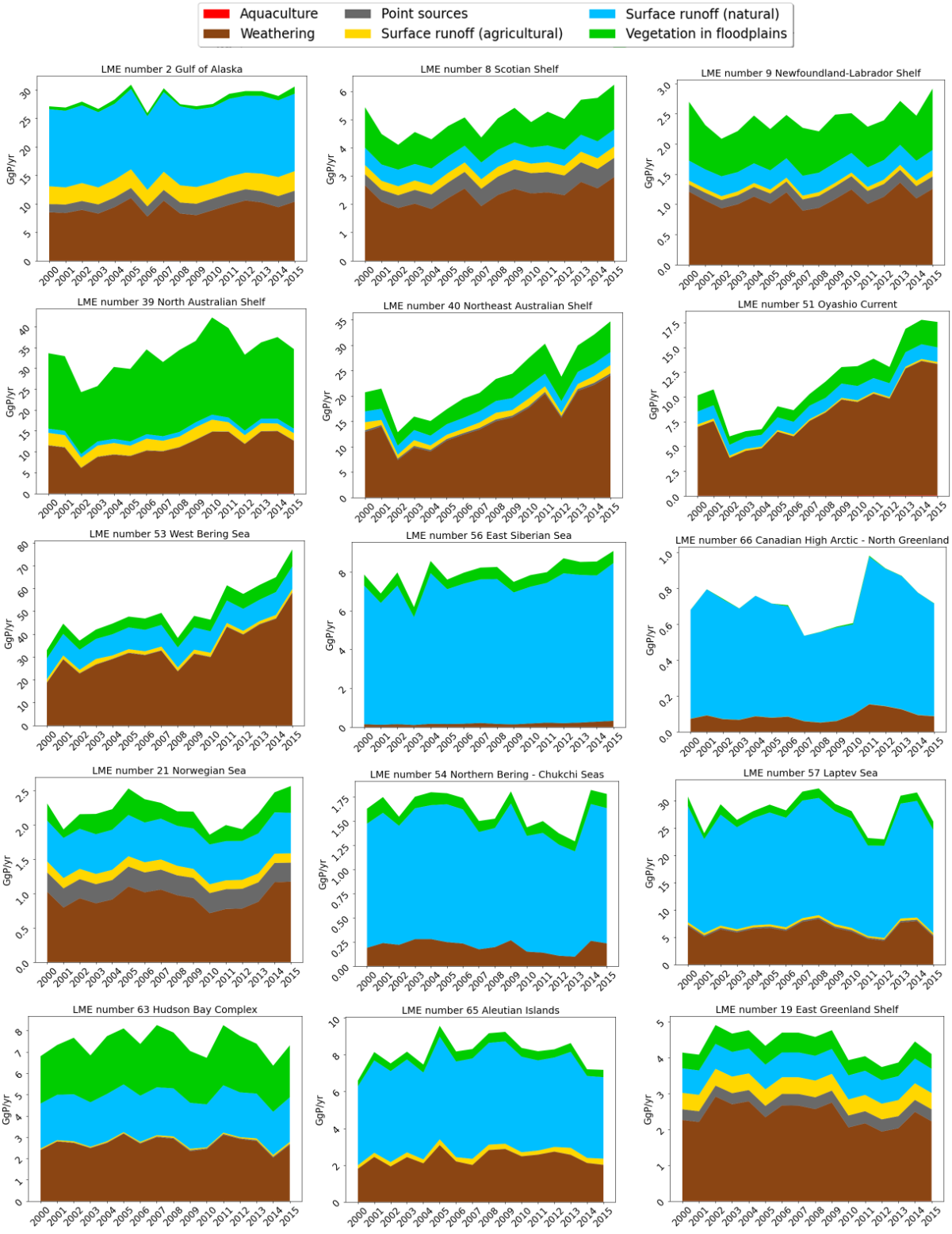

(To be continued on page 38)

(Following plots on page 37)

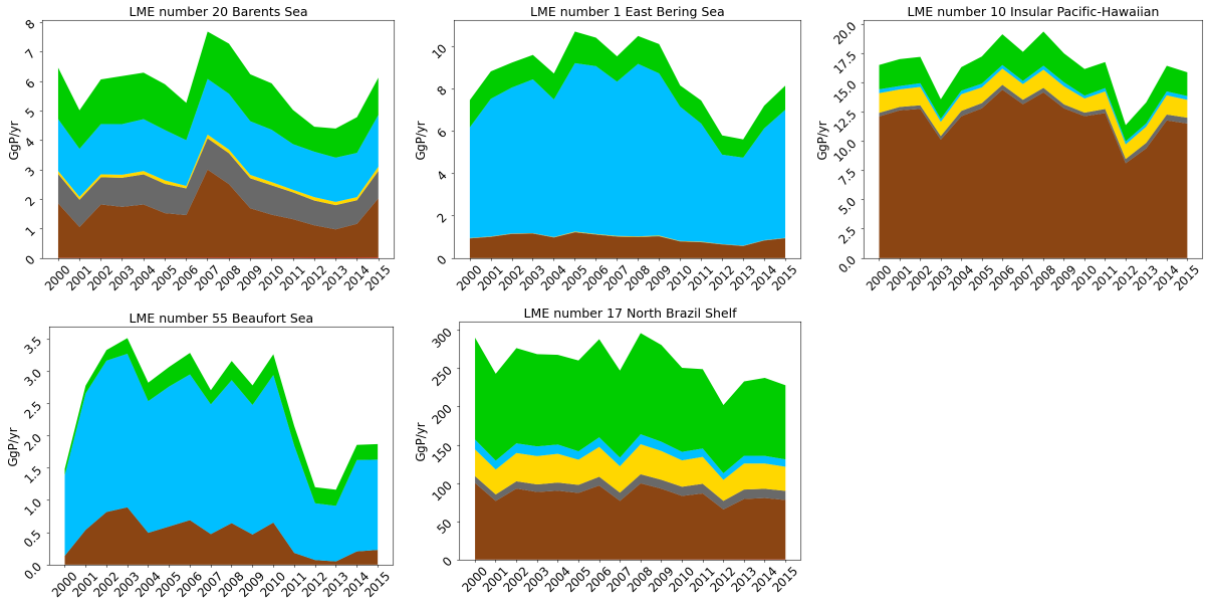

Figure 19. Long-term changes in river phosphorus export from 2000 to 2015 for LMEs with a dominance of natural sources in their river export. Twenty LMEs with this trend are shown.

4.2.4.2 LMEs with river export dominated by anthropogenic sources

In contrast, in thirty-four LMEs, human activities play a significant role as a dominant source of their received river P export (Figure 20). These LMEs are the California Current (3), the Gulf of California (4), the Gulf of Mexico (5), the Southeast U.S. Continental Shelf (6), the Northeast U.S. Continental Shelf (7), the Caribbean Sea (12), the Humboldt Current (13), the Patagonian Shelf (14), the South Brazil Shelf (15), the East Brazil Shelf (16), the North Sea (22), the Baltic Sea (23), the Celtic-Biscay Shelf (24), the Iberian Coastal (25), the Mediterranean Sea (26), the Canary Current (27), the Agulhas Current (30), the Somali Coastal Current (31), the Arabian Sea (32), the Red Sea (33), the Bay of Bengal (34), the Gulf of Thailand (35), the South China Sea (36), the East Central Australian Shelf (41), the Southeast Australian Shelf (42), the South West Australian Shelf (43), the West Central Australian Shelf (44), the Northwest Australian Shelf (45), the New Zealand Shelf (46), the East China Sea (47), the Yellow Sea (48), the Kuroshio Current (49), the Sea of Japan (50), the Sea of Okhotsk (52), and the Black Sea (62).

Twenty LMEs witnessed an increasing trend in total external P river export from 2000 to 2015, with a dominance of anthropogenic sources. For example, the Bay of Bengal (34) showed an increasing trend of 164 Gg P/yr in river export during the aforementioned period, with an average proportion of 61% from agricultural systems via surface runoff, 14% from point sources, 3% from aquaculture, and the rest from natural sources. The river P export to the Arabian Sea (32) increased by about 2 times during this period, with an average contribution of 69% from agricultural systems via surface runoff, 19% from point sources and the rest from other sources. The river P export to the South China Sea (36) demonstrated an increase of 68 Gg P/yr during the 2000-2015, with an average share of 43% from agricultural systems via surface runoff, 30% from point sources, 6% from aquaculture, and the rest from natural sources. For the East Central Australian Shelf (41), the river P export increased from 4 Gg/yr in 2000 to 7 Gg/yr in 2015, with an average contribution of 67% from point sources, 13% from agricultural systems via surface runoff, and the rest from

natural sources. The river P export to the East China Sea (47) increased by 31 Gg P/yr during this period, where point sources accounted for an average contribution of 51%, agricultural surface runoff accounted for 33%, aquaculture accounted for 8%, and the rest was from natural sources. The Yellow Sea (48) saw an increase of 238 Gg P/yr in river P export during the aforementioned period, with an average proportion of 52% from agricultural systems via surface runoff, 33% from point sources, 9% from aquaculture, and the rest from natural sources.

Four LMEs received stable river P export during 2000-2015, with a dominance of anthropogenic sources. For instance, the California Current (3) received an average of 46 Gg P/yr of river export during this period, with an average contribution of 52% from agricultural systems via surface runoff, 16% from point sources, and the rest from natural sources. The Gulf of Thailand (35) received an average of 23 Gg P/yr of river export during the aforementioned period, with an average proportion of 42% from agricultural surface runoff, 21% from point sources, 7% from aquaculture, and the rest from natural sources.

Ten LMEs witnessed a decreasing trend in river P export from 2000 to 2015, with a dominance of anthropogenic sources. For example, the Gulf of Mexico (5) received a decrease of 29 Gg P/yr in its river export during this period, with an average contribution of 56% from agricultural systems via surface runoff, 19 % from point sources, and the rest from natural sources. The river P export to the Humboldt Current (13) decreased from 67 Gg P/yr in 2000 to 46 Gg/yr in 2015, with an average proportion of 53% from agricultural systems via surface runoff, 18 % from point sources, and the rest from natural sources.

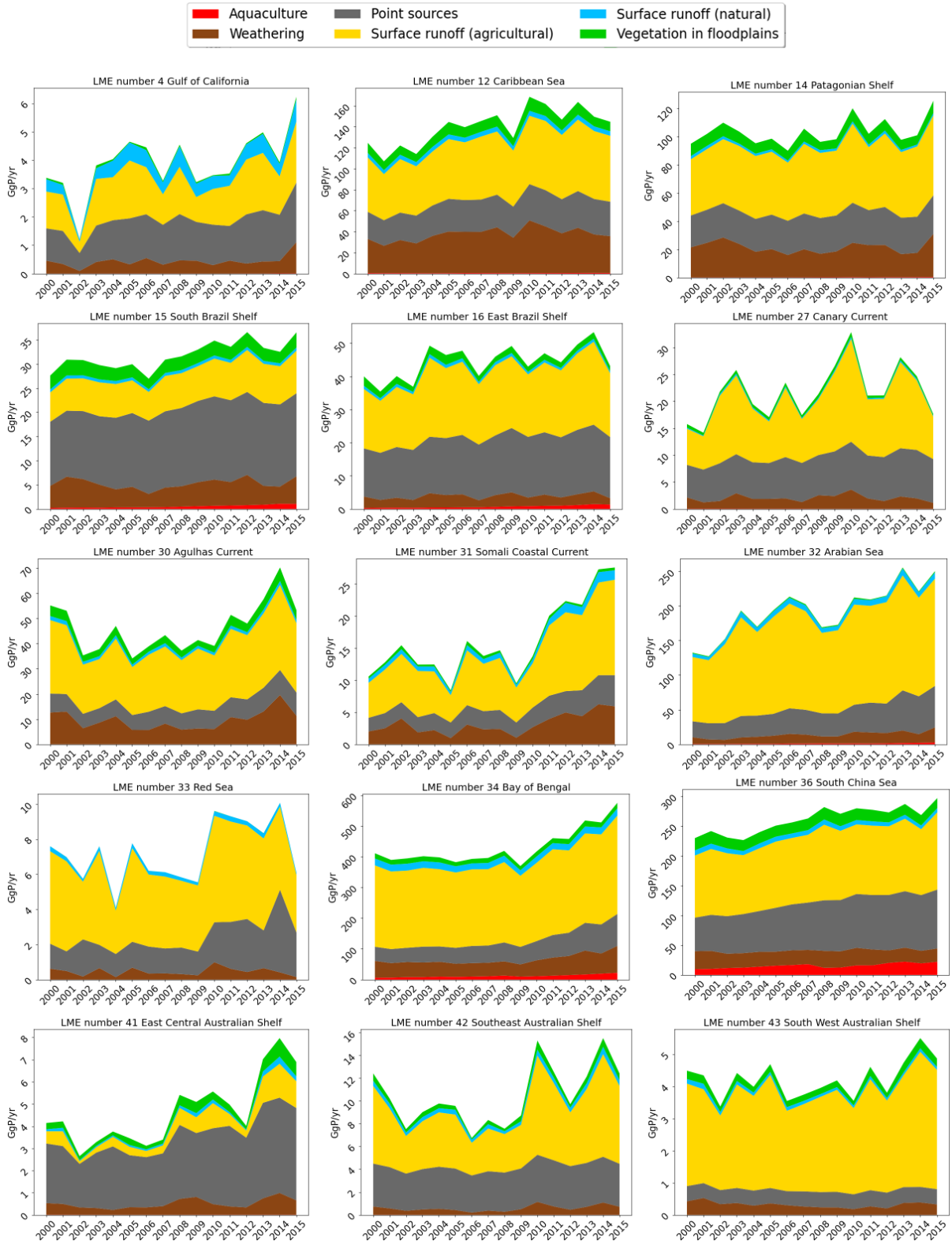

(To be continued on page 41)

(Following plots on page 40)

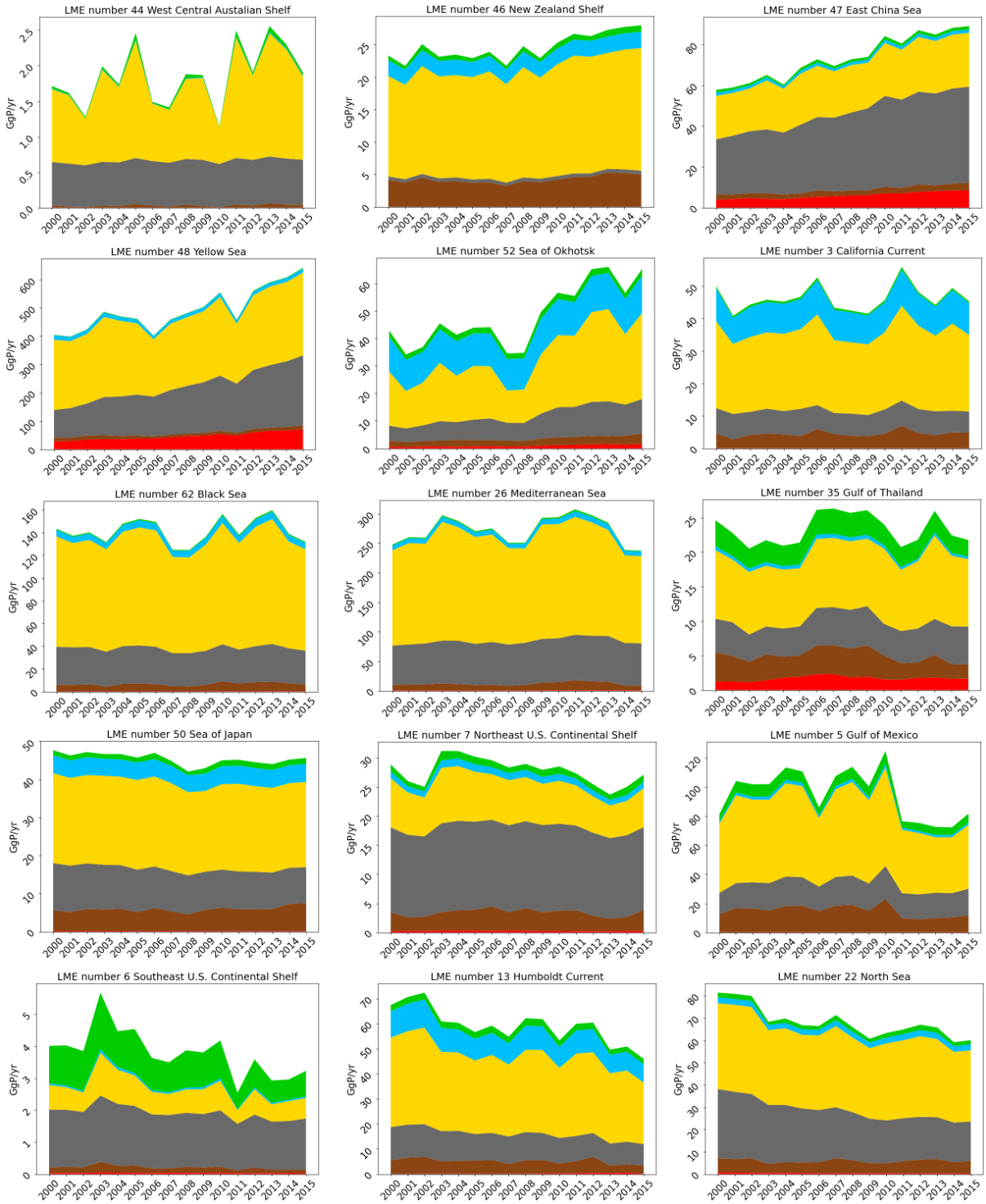

(To be continued page 42)

(Following plots on page 41)

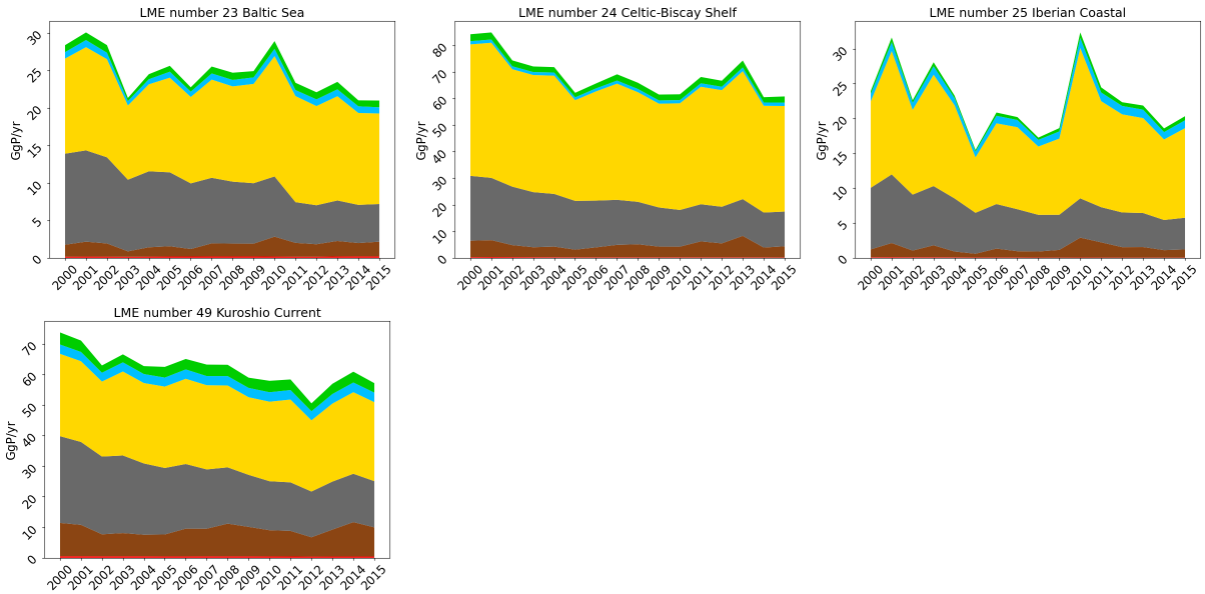

Figure 20. Long-term changes in river phosphorus export from 2000 to 2015 for LMEs with a dominance of anthropogenic sources in their river export.

4.2.4.3 LMEs with river export from similarly important anthropogenic and natural sources

In eight LMEs, both natural and anthropogenic sources are similarly important in river P export (Figure 21). These LMEs are the Pacific Central-American Coastal (11), the Guinea Current (28), the Benguela Current(29), the Sulu-Celebes Sea (37), the Indonesian Sea (38), the Northwest Australian Shelf (45), the Kara Sea (58), and the Faroe Plateau (60).

Five LMEs demonstrated an increasing trend in their received river P export during 2000-2015. For example, the river P export to the Guinea Current (28) increased from 78 Gg P/yr to 99 Gg/yr during 2000-2015, with an average contribution of 41% from natural sources and 59% from anthropogenic sources.

Two LMEs showed almost stable trends in their received river P export during 2000-2015. For instance, the Kara Sea (58) received an average of 52 Gg P/yr of river export during the aforementioned period, with an average proportion of 43% from natural sources and 57% from anthropogenic sources.

One LME, the Faroe Plateau (60), received decreasing river P export from 0.28 Gg P/yr to 0.24 Gg/yr during 2000-2015, decreased with an average contribution of 55% from natural sources and 45% from anthropogenic sources.

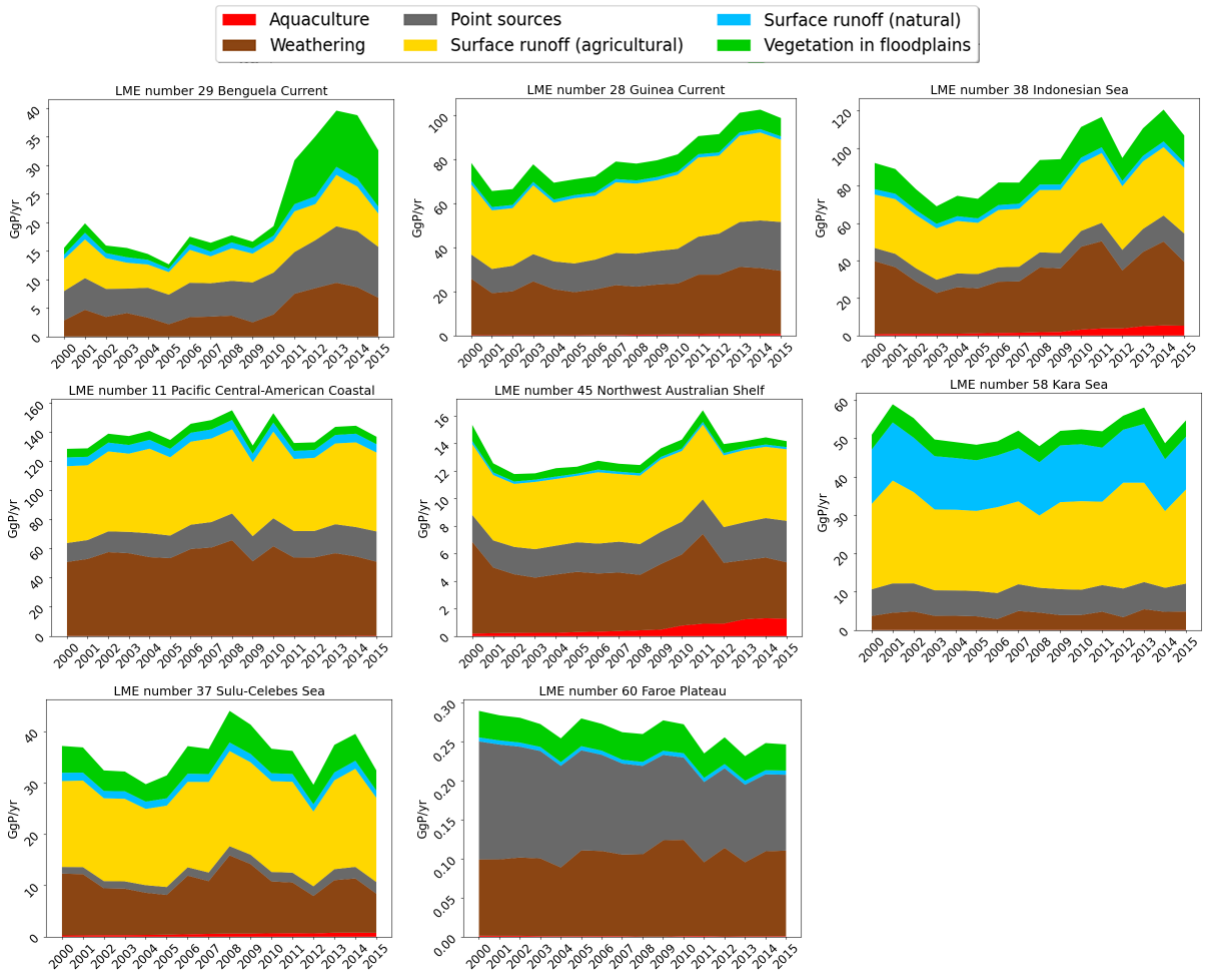

Figure 21. Long-term changes in river phosphorus export from 2000 to 2015 for LMEs with a dominance of both natural and anthropogenic sources in their river export.

4.3. Molar TN:TP ratios in the total external nutrient inputs

4.3.1 LMEs with molar TN:TP ratios in nutrient inputs exceeding the Redfield ratio

The molar TN:TP ratios of nutrient inputs to forty-nine LMEs generally exceeded the Redfield N:P ratio of 16 during the period of 2000-2015 (Figure 22). These LMEs are the East Bering Sea (1), the Gulf of Alaska (2), the California Current (3), the Gulf of California (4), the Gulf of Mexico (5), the Southeast U.S. Continental Shelf (6), the Northeast U.S. Continental Shelf (7), the Scotian Shelf(8), the Newfoundland-Labrador Shelf (9), the Insular Pacific-Hawaiian (10), the Patagonian Shelf (14), the South Brazil Shelf (15), the East Brazil Shelf (16), the North Brazil Shelf (17), the East Greenland Shelf (19), the Barents Sea (20), the Norwegian Sea (21), the North Sea (22), the Baltic Sea (23), the Celtic-Biscay Shelf (24), the Iberian Coastal (25), the Benguela Current(29), the Agulhas Current (30), the Bay of Bengal (34),the Gulf of Thailand (35), the South China Sea (36), the Sulu-Celebes Sea (37), the Indonesian Sea (38), the North Australian Shelf (39), the Northeast Australian Shelf (40), the East Central Australian Shelf (41), the Southeast Australian Shelf (42), the South West Australian Shelf (43), the West Central Australian Shelf (44), the Northwest Australian Shelf (45), the New Zealand Shelf (46), the East China Sea (47), the Yellow Sea (48), the Kuroshio Current (49), the Sea of Japan (50), the Oyashio Current (51), the Sea of Okhotsk (52), the Northern Bering - Chukchi

Seas (54), the Kara Sea (58), the Faroe Plateau (60) the Black Sea (62), the Hudson Bay Complex (63), the Aleutian Islands (65), and the Canadian High Arctic - North Greenland (66).

The molar TN:TP ratios of nutrient inputs to nineteen LMEs demonstrated an increasing trend from 2000 to 2015 (Figure 22). The molar TN:TP ratio of the nutrient inputs to the Benguela Current (29) showed a dramatic increase from 21 in 2000 to 30 in 2015. The molar TN:TP ratio of the nutrient inputs to the Bay of Bengal (34) continuously increased from 24 to 35 during 2000-2015.

The molar TN:TP ratios of nutrient inputs to twelve LMEs showed no obvious increases or decreases from 2000 to 2015 (Figure 22). For example, in nutrient inputs to the Gulf of California (4), the TN to TP molar ratio was around 16.5 during this period. Similarly, the molar TN:TP ratio of nutrient inputs to the East China Sea (47) were around 35.2 during this period.

The molar TN:TP ratios of nutrient inputs to nineteen LMEs experienced a decreasing trend from 2000 to 2015 (Figure 22). For example, the molar TN:TP ratio of nutrient inputs to the Norwegian Sea (21) decreased

from 43 in 2000 to 32 in 2015. The molar TN:TP ratio of nutrient inputs to the Northeast Australian Shelf (40) decreased from up to 28 in the early 2000s to 18 in 2015.

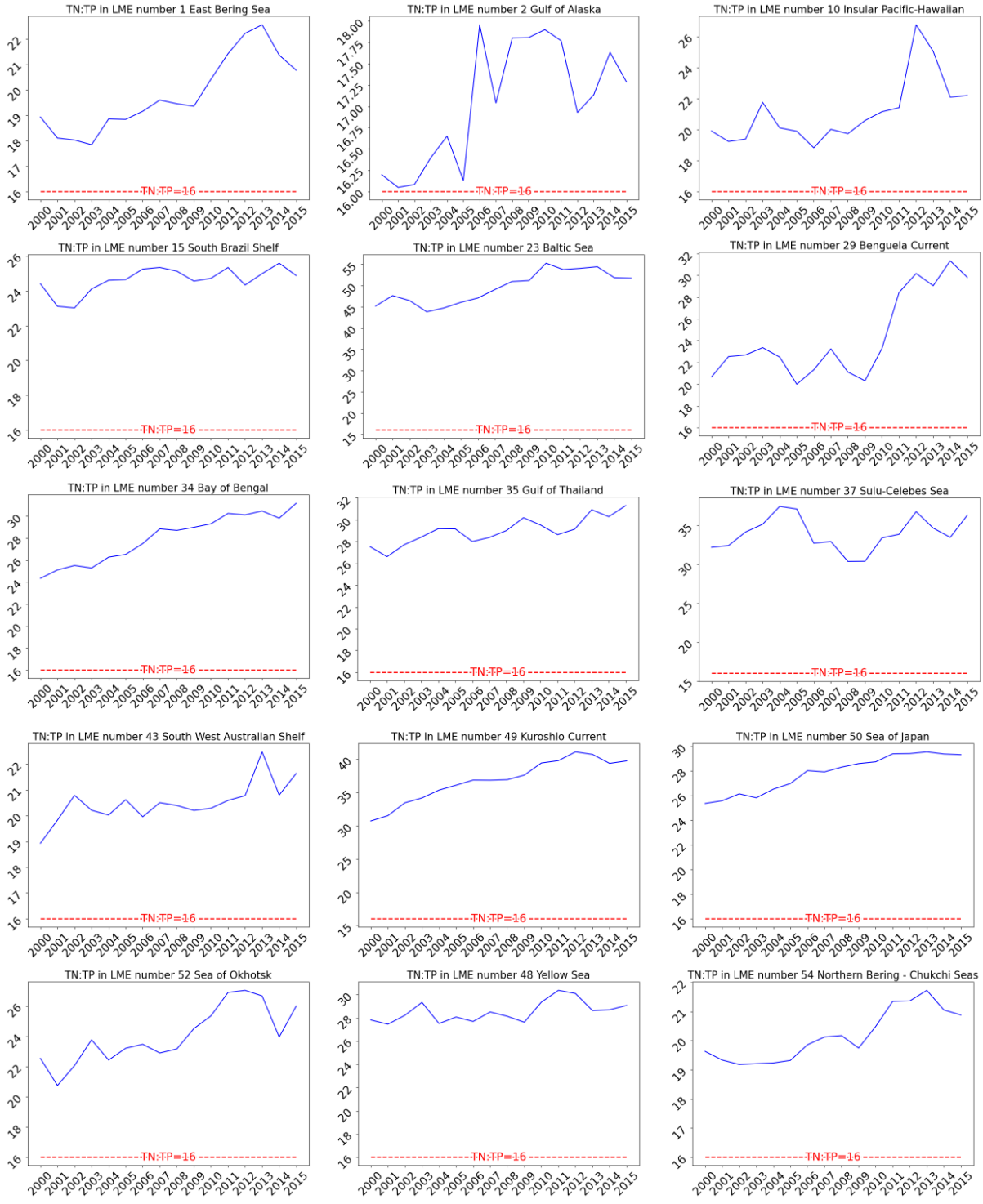

(To be continued on page 46)

(Following plots on page 45)

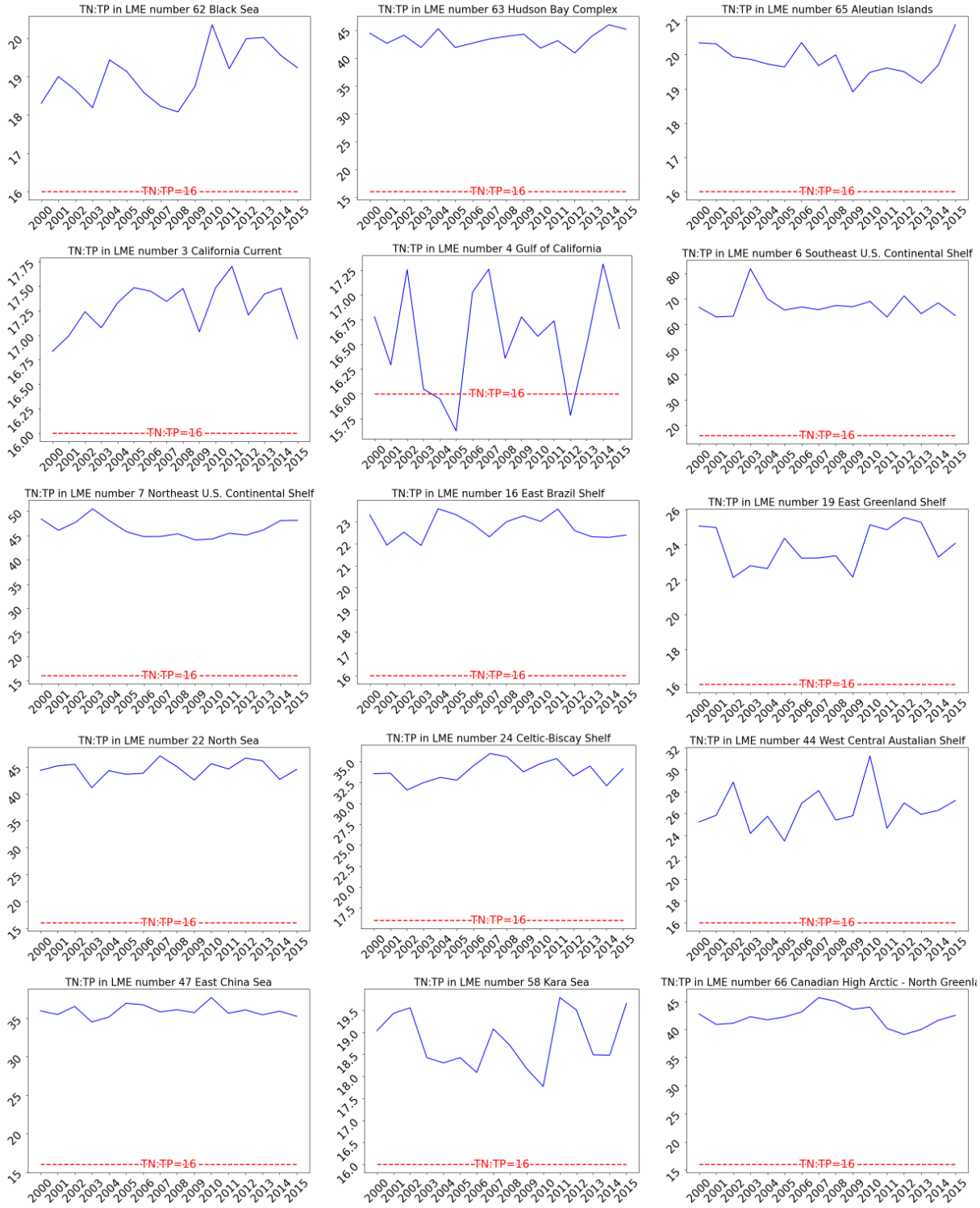

(To be continued on page 47)

(Following plots on page 46)

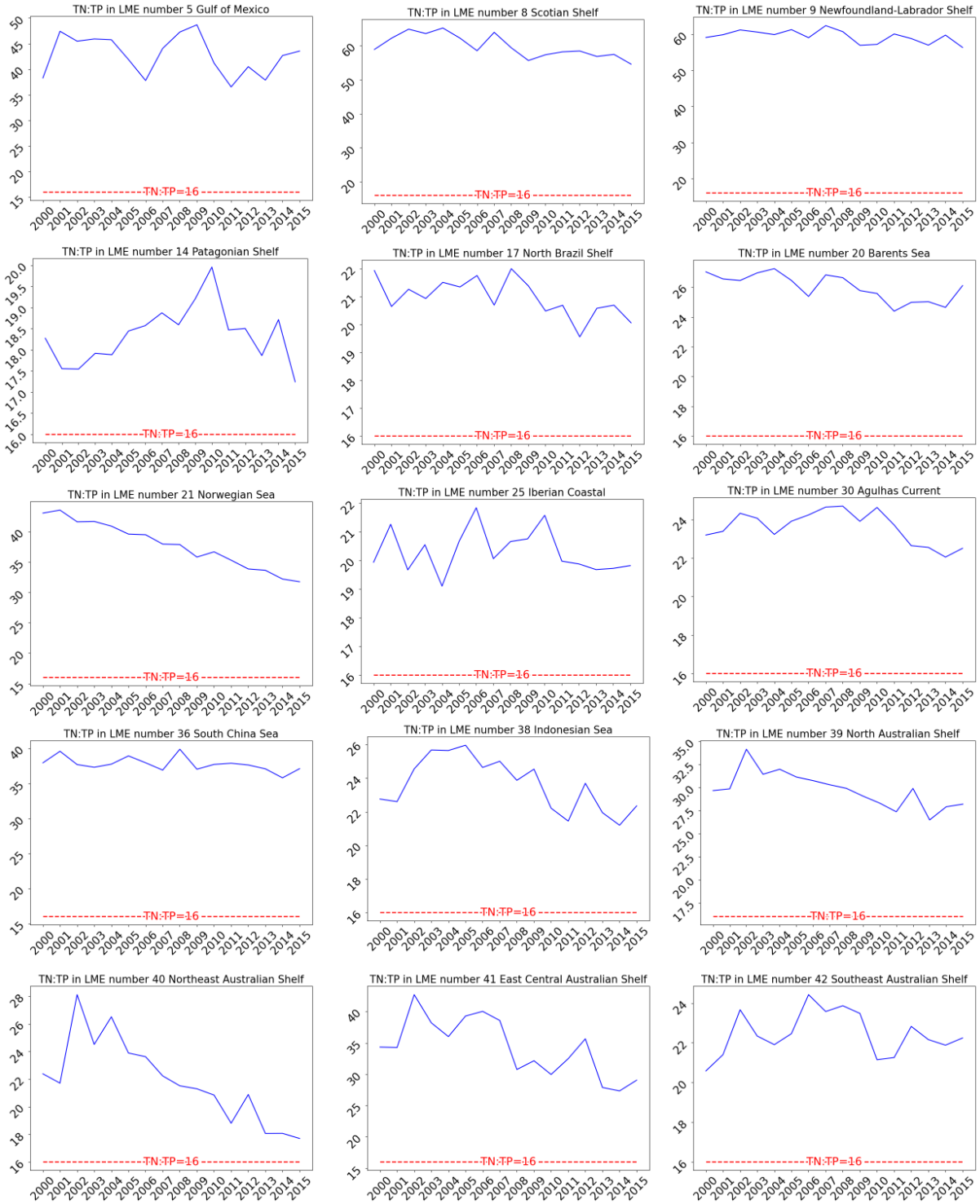

(To be continued on page 48)

(Following plots on page 47)

Figure 22. Long-term changes in the molar TN: TP ratio of nutrient inputs, for the LMEs whose TN:TP ratios remained above the Redfield ratio (16:1) during 2000-2015.

4.3.2 LMEs with increasing molar TN:TP in nutrient inputs from below to exceeding the Redfield ratio

The molar TN:TP ratios of nutrient inputs to three LMEs rapidly increased from below the Redfield ratio to over the Redfield ratio during 2000-2015 (Figure 23). The molar TN:TP ratio of nutrient inputs to the Humboldt Current (13) increased from around 14 to nearly 17.5, while TN:TP of nutrient inputs to the Beaufort Sea (55) grew from 15-16 in the 2000s to 19-20 in the early 2010s. The molar TN:TP ratio of the nutrient inputs to the East Siberian Sea (56) are generally below the Redfield Ratio during 2000s and the early 2010s, and started to exceed the Redfield ratio in 2015.

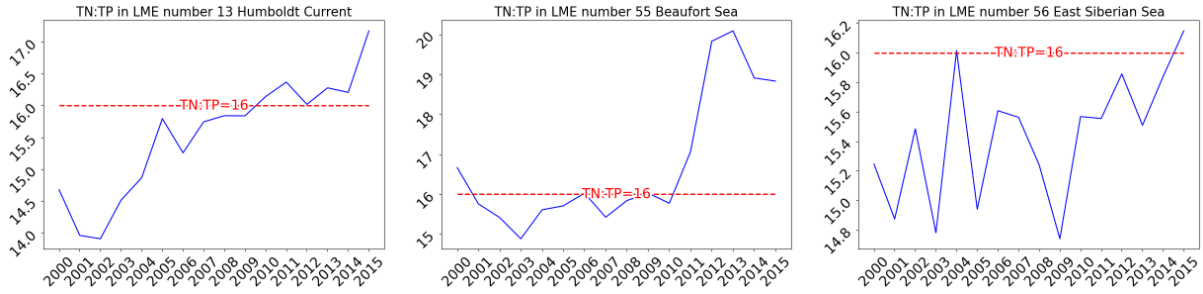

Figure 23. Long-term changes in the molar TN: TP ratio of nutrient inputs, for the LMEs whose TN:TP ratios increased from below to exceeding the Redfield ratio (16:1) during 2000-2015.

4.3.3 LMEs with molar TN:TP in nutrient inputs below the Redfield ratio

The molar TN:TP ratios of nutrient inputs to ten LMEs were lower than the Redfield N:P ratio of 16 during 2000-2015 (Figure 24). These LMEs are the Pacific Central-American Coastal (11), the Caribbean Sea (12), the Mediterranean Sea (26), the Canary Current (27), the Guinea Current (28), the Somali Coastal Current (31), the Arabian Sea (32), the Red Sea (33), the West Bering Sea (53), the Laptev Sea (57).

Among these ten LMEs, the molar TN:TP ratios of nutrient inputs to five LMEs demonstrated an increasing trend during 2000-2015. For example, the molar TN:TP ratio of nutrient inputs to the Guinea Current (28) increased from 8 in 2000 to 10 in 2015, while those in the Somali Coastal Current (31) and the Arabian Sea (32) both experienced a gradual increase, reaching nearly 6 in 2015.

The molar TN:TP ratios of nutrient inputs to four LMEs were stable during 2000-2015. For instance, that in the Red Sea (33) were very low of around 1 during this period, while those in the Mediterranean Sea (26) ranged between 9 and 10.

The molar TN:TP ratio of nutrient inputs decreased in only one LME, the West Bering Sea (53), from 15 in 2000 to 11 in 2015.

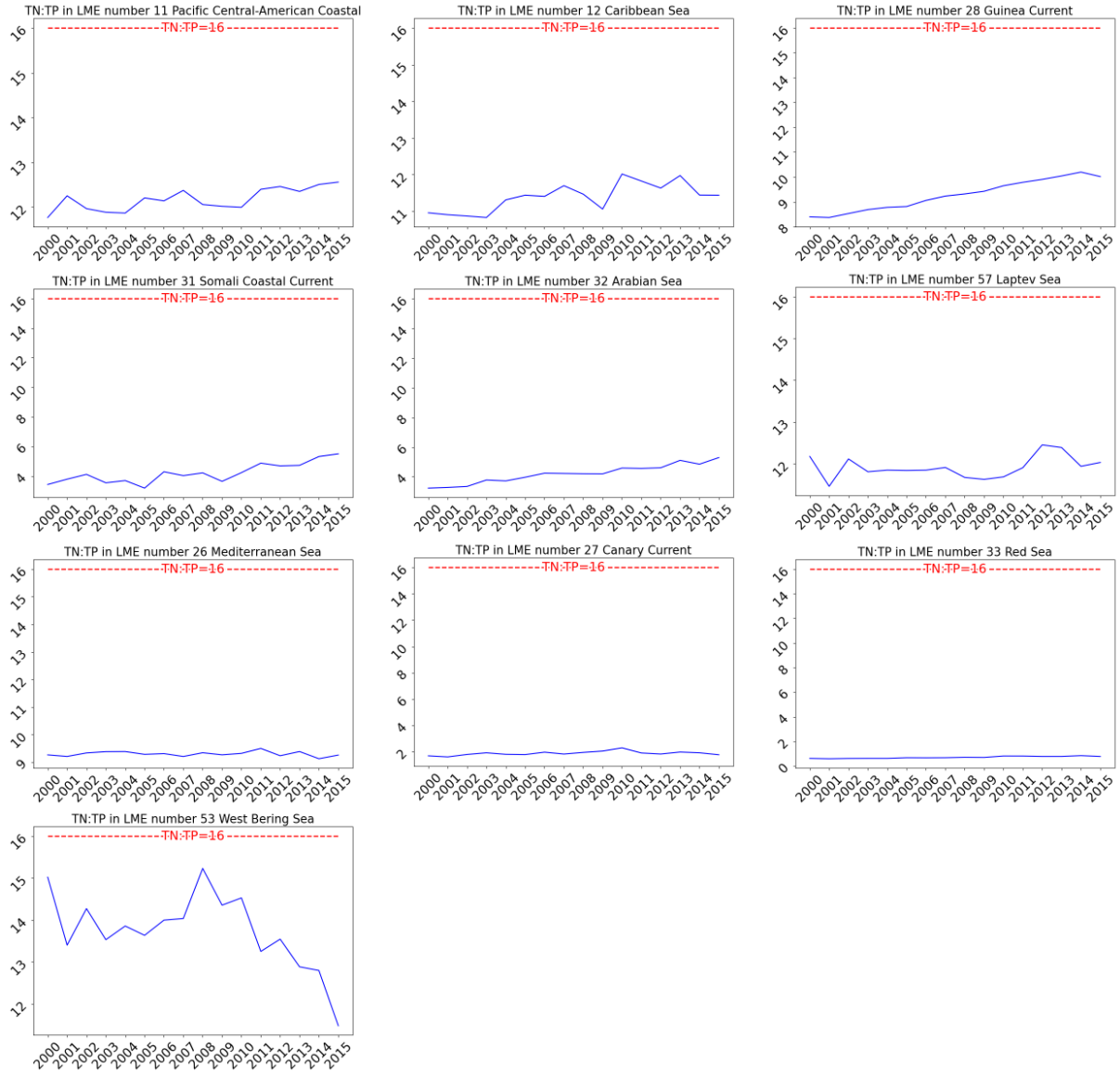

Figure 24. Long-term changes in the molar TN:TP ratio of nutrient inputs, for the LMEs whose TN:TP ratios remained below the Redfield ratio (16:1) during 2000-2015.

4.4 Relationships between the molar TN: TP ratios in nutrient inputs vs. annual coastal algal bloom frequencies

In this study, the correlation relationships between the ratios of TN:TP in nutrient inputs and the frequencies of coastal algal blooms across 62 LMEs from 2000 to 2015 were investigated.

Twenty-seven LMEs showed a positive correlation relationship of the TN:TP ratio in their nutrient inputs vs. their annual coastal algal bloom frequency during 2000-2015 (Figure 25). These LMEs are the East Bering Sea (1), the California Current (3), the Gulf of Mexico (5), the Newfoundland-Labrador Shelf (9), the Pacific Central-American Coastal (11), the Humboldt Current (13), the Patagonian Shelf (14), the South Brazil Shelf (15), the North Brazil Shelf (17), the East Greenland Shelf (19), the North Sea (22), the Baltic Sea (23), the

Iberian Coastal (25), the Benguela Current (29), the Somali Coastal Current (31), the Arabian Sea (32), the Indonesian Sea (38), the Northeast Australian Shelf (40), the East Central Australian Shelf (41) the South West Australian Shelf (43), the Northwest Australian Shelf (45), the Yellow Sea (48), the Sea of Japan (50), the Sea of Okhotsk (52), the Northern Bering - Chukchi Seas (54), the Kara Sea (58), and the Aleutian Islands (65). Twenty-four (about 90%) of these LMEs had TN:TP ratios in their nutrient inputs high than the Redfield Ratio of 16.

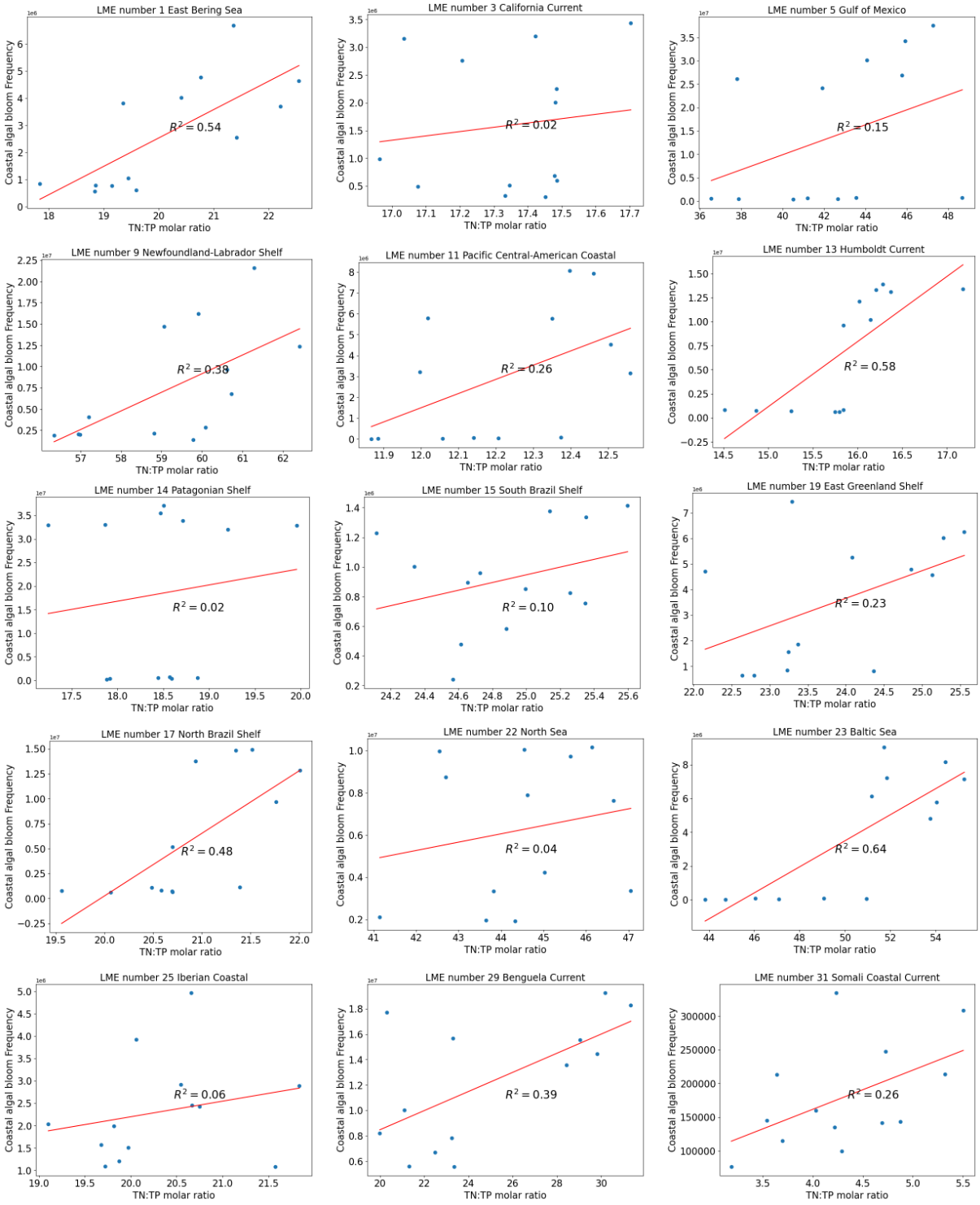

(To be continued on page 53)

(Following plots on page 52)

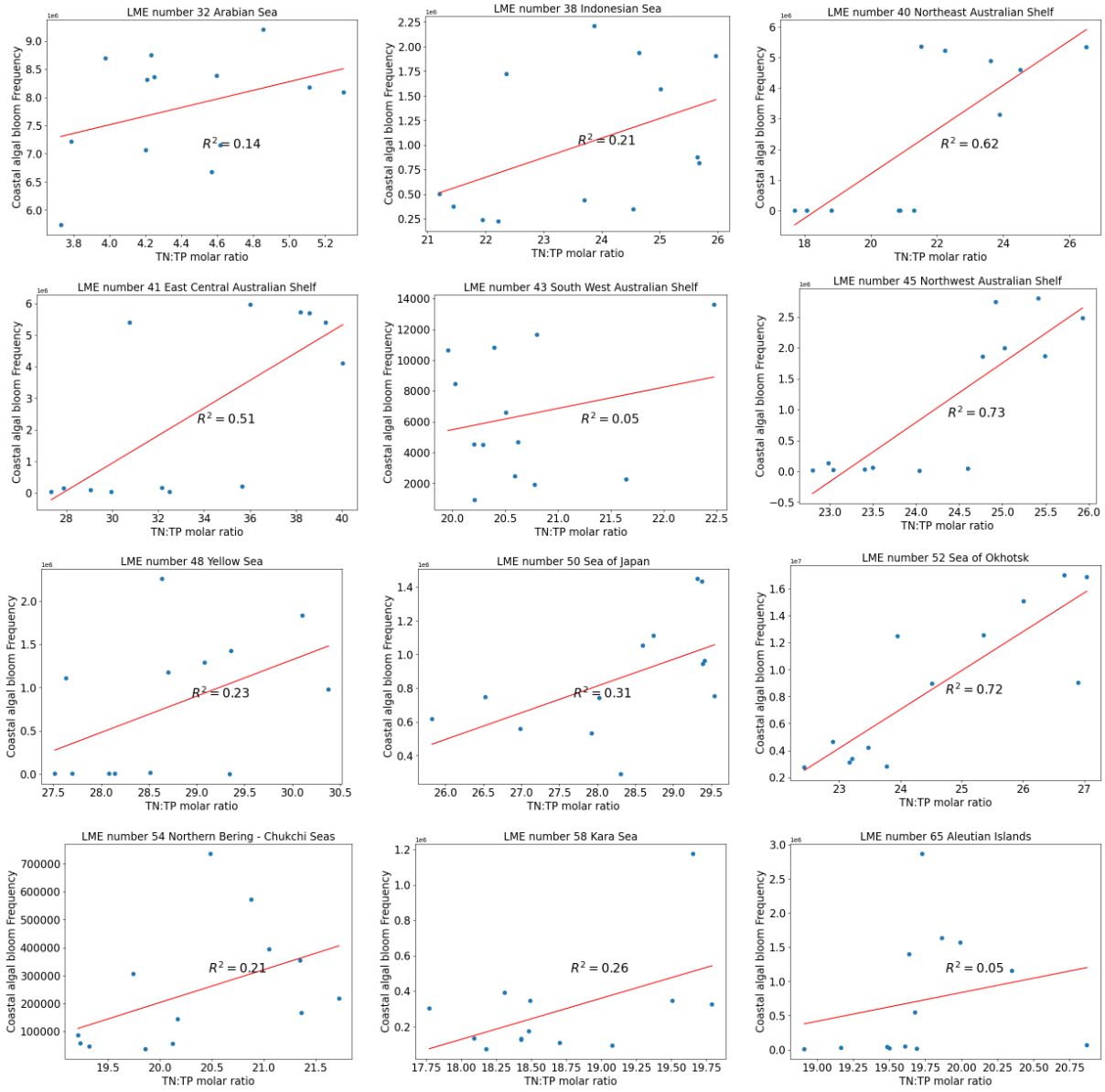

Figure 25. LMEs with positive correlation relationships between the molar TN:TP ratios in nutrient inputs and annual coastal algal bloom frequencies during 2000-2015.

Twenty-nine LMEs showed a negative correlation of TN:TP ratios in their nutrient inputs vs. their annual coastal algal bloom frequency during 2000-2015 (Figure 26). These LMEs are the Gulf of Alaska (2), the Southeast U.S. Continental Shelf (6), the Northeast U.S. Continental Shelf (7), the Scotian Shelf(8), the Insular Pacific-Hawaiian (10), the Caribbean Sea (12), the Barents Sea (20), the Norwegian Sea (21), the Canary Current (27), the Guinea Current (28), the Agulhas Current (30), the Red Sea (33), the Bay of Bengal (34), the Gulf of Thailand (35), the South China Sea (36), the North Australian Shelf (39), the Southeast Australian Shelf (42), the West Central Australian Shelf (44), the New Zealand Shelf (46), the East China Sea (47), the Kuroshio Current (49), the Oyashio Current (51), the West Bering Sea (53), the Beaufort Sea (55),

the Laptev Sea (57), the Faroe Plateau (60), the Black Sea (62), the Hudson Bay Complex (63), and the Canadian High Arctic - North Greenland (66). The peak algal bloom frequencies occurred at different TN:TP ratios in different LMEs, which indicate that different species with different preferred N: P ratios may dominate the algal blooms in different LMEs.

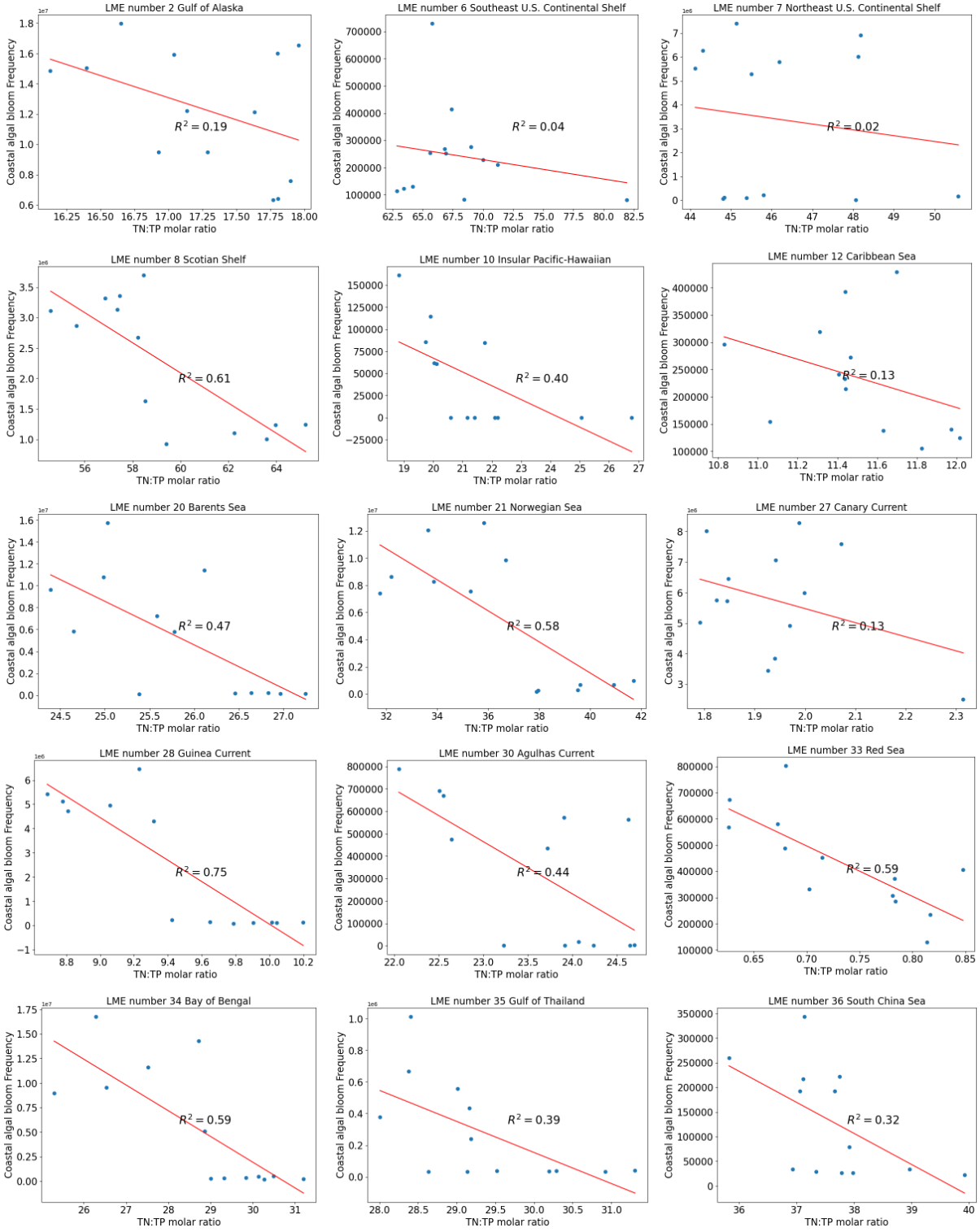

(To be continued on page 55)

(Following plots on page 54)

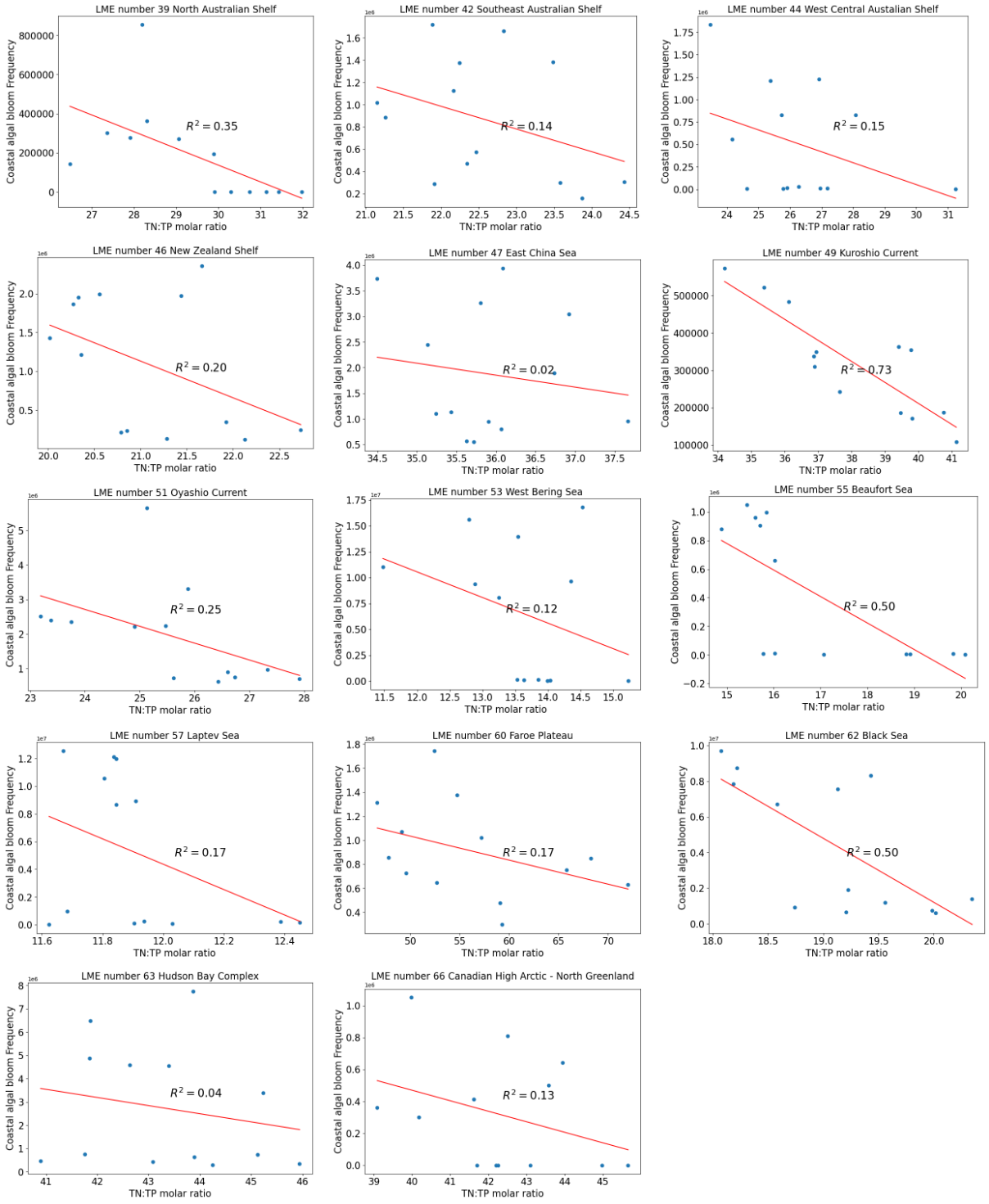

Figure 26. LMEs with negative correlation relationships between the molar TN: TP ratios in nutrient inputs and annual coastal algal bloom frequencies during 2000-2015.

Six LMEs demonstrated no significant positive or negative correlation relationships between the TN: TP ratios in nutrient inputs and their annual coastal algal bloom frequencies during 2000-2015 (Figure 27). These LMEs are the Gulf of California (4), the East Brazil Shelf (16), the Celtic-Biscay Shelf (24), the Mediterranean Sea (26), the Sulu-Celebes Sea (37), and the East Siberian Sea (56).

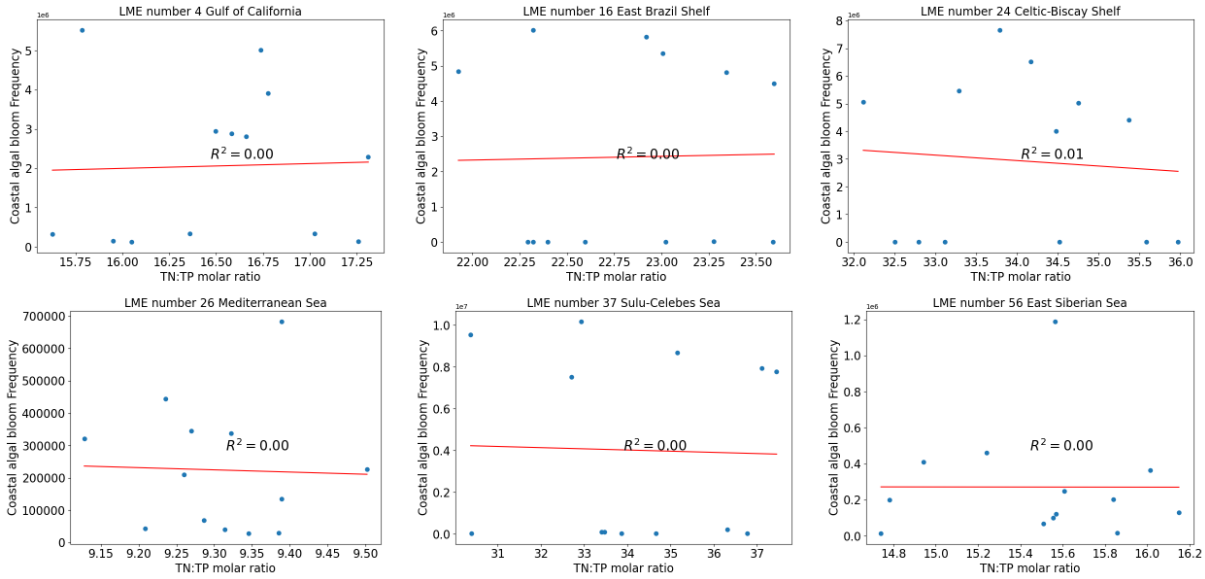

Figure 27. LMEs with no obviously correlation relationships between the molar ratios of TN: TP ratios in nutrient inputs and annual coastal algal bloom frequencies during 2000-2015.

5. Discussion

5.1 Total Nitrogen and Phosphorus Input to Coastal Waters

Inputs of nutrients, particularly N and P, resulting in eutrophication and algal blooms in coastal areas (Yu and Liu, 2016; Wang et al, 2020a), which may consequently lead to hypoxia and negative impacts on the fisheries industry and human health (Anderson et al., 2002). Several factors have accelerated this phenomenon, including population growth, increased agricultural production and its nutrient use, and the expansion of mariculture in recent years (Yu et al., 2018; Li et al., 2021).

Our results reveal diverse trends in the total external N and P inputs across different LMEs during the period 2000-2015 from sources of river export, atmospheric deposition, mariculture, and submarine fresh groundwater discharge. These trends reflect variations among LMEs in terms of ecological and geological features, geographical locations, population, land-use land cover, food production activities, and economic growth in their bordering land systems. Most of the LMEs, namely thirty-three for N and thirty-two for P, demonstrated an increase in their nutrient inputs during the period 2000-2015 (Figures 3, 4,12, 13-14). The total N inputs were stable in twenty-one LMEs and the total P inputs were stable in seventeen LMEs (Figures 5, 6, 15-16). Eight LMEs had decreased total external N inputs and thirteen LMEs had decreased total external P inputs (Figures 7, 8, 17-18) during the aforementioned period.

From the main sources of total N and P inputs, river export, and atmospheric deposition are the main contributors, with an average combined contribution of 85-100% for total N inputs and 62-100% for total P

inputs during the period 2000-2015. Mariculture and submarine fresh groundwater discharge are minor contributors in most LMEs. However, in LMEs such as the Norwegian Sea (21) and the Faroe Plateau (60), the recent contributions from mariculture are considerable for both N and P inputs. Our results show that the contribution of mariculture has become more significant in recent years. River export, atmospheric deposition and mariculture should be a focus of pollution control in these LMEs.

5.2 Sources of Nitrogen and Phosphorus in River Export

We grouped the sources of N and P in river export into two parts: natural and anthropogenic. This research shows that the role of anthropogenic is significant in 32 LMEs for river N export and in 34 LMEs for river P export. Most of them showed increases during 2000-2015. This causes more nutrient load in river export to coastal systems, which consequently affects water quality and biodiversity (Beusen et al., 2022).

Twenty-one LMEs had river N export with a dominance of natural sources (Figure 9), thirty-two LMEs dominated anthropogenic sources in their river N export (Figure 10), and nine LMEs had river N export with a dominance of both natural and anthropogenic sources (Figure 11). For river P export, twenty LMEs showed a dominance of natural sources (Figure 19), 34 LMEs dominated anthropogenic sources (Figure 20), and 8 LMEs dominated both natural and anthropogenic sources (Figure 21).

Overall, the average contributions of natural sources to river N and P export are about 44% and 43% for all LMEs, respectively, while the average contributions of anthropogenic sources to river N and P export are about 56% and 57%, respectively. Among natural sources, groundwater and vegetation in floodplains are the most important contributors to river N export, while surface runoff and weathering are the most significant for river P export. From anthropogenic sources, agricultural land use and wastewater discharge are the largest contributors to river N and P export, acting as important nutrient sources (de Wit et al., 2002; Bouwman et al., 2009; Morée et al., 2013; Bouwman et al., 2013; van Puijenbroek et al., 2019). Moreover, the contribution of aquaculture has become more important in recent years in river nutrient export to some LMEs (Wang et al., 2020b).

5.3 Relationships Between Molar TN: TP Ratio and Frequency of Coastal Algal Blooms (HABs)

Studies show that there appears to be a potential relationship between algal blooms and eutrophication on a global scale (Glibert and Burkholder, 2008). Research conducted by Anderson et al. (2002), Heisler et al. (2008), and Wang et al. (2019) suggests that increased N inputs relative to P inputs in coastal areas can disrupt nutrient ratios and alter nutrient stoichiometry to be away from the Redfield ratio, resulting in the preferential nutrient utilization by certain species that contribute to the emergence of harmful algal blooms when other environmental conditions are favorable.

The relationship between aggregated molar TN: TP ratios in nutrient inputs and the occurrence of HABs in Chinese coastal areas has been investigated. Analysis reveals that in certain LMEs, higher HAB occurrences correlate with increased N inputs and started to proliferate when exceeding the critical thresholds of molar TN: TP ratios of 25 or 30 in the Yellow Sea, East China Sea and South China Sea (Wang et al., 2021).

Chen et al. (2013) suggest that N and P are the primary nutrients that can limit and support the occurrence of eutrophication and HABs. By comparing TN:TP ratio with the nutrient uptake ratio by general marine phytoplankton, known as the Redfield ratio (C:N:P=106:16:1) (Fujimoto et al., 1997), we can understand the nutrient limitation for algal growth.

Our result demonstrated in most LMEs, the molar TN: TP ratios of nutrient inputs increased and remained above the Redfield ratio (Figure 22). Conversely, some LMEs exhibited TN:TP ratios in their nutrient inputs below the Redfield ratios, but their ratios increased during 2000-2015 (Figures 23-24). When the N inputs increased faster than the P inputs in the coastal area, or when the P inputs decreased faster than the N inputs, the TN:TP ratio in nutrient inputs increased.

The correlation analyses of coastal algal bloom frequency and TN:TP ratios in their nutrient inputs show that in twenty-seven LMEs, higher algal bloom frequencies occurred with higher TN: TP ratios in nutrient inputs (Figure 25). Such nutrient conditions become more suitable for certain algae species. When TN: TP ratios in inputs exceed threshold values of nutrient ratios, they induce changes in phytoplankton composition and dominant species, as well as associated algal growth (Tang et al., 2003; Wang, 2006; Ning et al., 2010). For example, Marshall et al. (2009) observed a shift from diatoms to flagellates in the Chesapeake Bay, United States.

On the other hand, in twenty-nine LMEs, there was negative correlations or no significant correlations between molar TN: TP ratios in nutrient inputs and coastal algal bloom frequencies (Figures 26-27). In these LMEs, the peak algal bloom frequencies occurred at different TN:TP ratios for different LMEs, which indicate that different species with different preferred N: P ratios may dominate the algal blooms in different LMEs, and the other environmental conditions besides nutrients may have impacts on the local algal blooms. This indicates that the use of the N:P ratio as the only factor to predict the occurrence of algal blooms remains uncertain due to factors such as water residence times, temperature, and light availability in specific regions (Painting et al., 2007; Xiao et al., 2019).

6. Conclusion

During the period 2000-2015, about half of the LMEs showed increases in their total external N and P inputs, with river export and atmospheric deposition as the dominant contributors and mariculture and submarine fresh groundwater discharge as minor contributors. In riverine N and P export, anthropogenic sources from agricultural lands, wastewater discharge of urban and rural areas, and aquaculture play significant roles in the increase in N and P river export to the LMEs dominated by human activities. Among natural sources of N and P river export, loads from natural systems via groundwater, floodplain vegetation for N, and weathering and loads from natural systems via surface runoff for P are the dominant contributors. Despite the small proportions of mariculture in some LMEs, its significance has grown in recent years, particularly for some LMEs.

The molar TN: TP ratio in nutrient inputs to LMEs increased and exceeded the Redfield ratio in many LMEs, which concurred with higher annual frequencies of coastal algal blooms. As increased or persistently high nutrient inputs and imbalanced N:P ratios lead to a heightened risk of coastal algal blooms (HABs) (Wang et al., 2021), there is an urgent need to mitigate N and P pollution through nutrient reduction strategies that take into consideration N:P ratios.

7. Reference

Anderson, D., Burkholder, J., Cochlan, W., Glibert, P., Gobler, C., Heil, C., Kudela, R., Parsons, M., Rensel, J., Townsend, D., Trainer, V., & Vargo, G. (2008). Harmful algal blooms and eutrophication: Examining linkages from selected coastal regions of the United States. Harmful Algae, 8, 39–53. https://doi.org/10.1016/j.hal.2008.08.017

Anderson, D. M., Glibert, P. M., & Burkholder, J. M. (2002). Harmful algal blooms and eutrophication: Nutrient sources, composition, and consequences. Estuaries, 25(4), 704–726. https://doi.org/10.1007/BF02804901

Beusen, A. H. W., Doelman, J. C., Van Beek, L. P. H., Van Puijenbroek, P. J. T. M., Mogollón, J. M., Van Grinsven, H. J. M., Stehfest, E., Van Vuuren, D. P., & Bouwman, A. F. (2022). Exploring river nitrogen and phosphorus loading and export to global coastal waters in the Shared Socio-economic pathways. *Global Environmental Change*, *72*, 102426. https://doi.org/10.1016/j.gloenvcha.2021.102426

Beusen, A. H. W., Bouwman, A. F., Van Beek, L. P. H., Mogollón, J. M., & Middelburg, J. J. (2016). Global riverine N and P transport to ocean increased during the 20th century despite increased retention along the aquatic continuum. Biogeosciences, 13(8), 2441–2451. https://doi.org/10.5194/bg-13-2441-2016

Beusen, A. H. W., Van Beek, L. P. H., Bouwman, A. F., Mogollón, J. M., & Middelburg, J. J. (2015). Coupling global models for hydrology and nutrient loading to simulate nitrogen and phosphorus retention in surface water. Description of IMAGE-GNM and analysis of performance. Geoscientific Model Development, 8(4), 4045–4067. https://doi.org/10.5194/gmd-8-4045-2015

Bouwman, A. F., Beusen, A. H. W., Glibert, P. M., Overbeek, C. C., Pawlowski, M., Herrera, J., et al. (2013). Mariculture: Significant and expanding cause of coastal nutrient enrichment. Environmental Research Letters, 8(4), 044026. https://doi.org/10.1088/1748-9326/8/4/ 044026

Bouwman, Alexander, M. Pawłowski, Cheng Liu, A. Beusen, Sandra Shumway, P. Glibert, and Ciska Overbeek. “Global Hindcasts and Future Projections of Coastal Nitrogen and Phosphorus Loads Due to Shellfish and Seaweed Aquaculture.” Reviews in Fisheries Science 19 (October 1, 2011): 331–57. https://doi.org/10.1080/10641262.2011.603849.

Bouwman, A.F., Beusen, A. H. W., & Billen, G. (2009). Human alteration of the global nitrogen and phosphorus soil balances for the period 1970–2050. Global Biogeochemical Cycles, 23, GB0A04. https://doi.org/10.1029/2009GB003576.

Brahney, J., Mahowald, N., Ward, D. S., Ballantyne, A. P., & Neff, J. C. (2015). Is atmospheric phosphorus pollution altering global alpine Lake stoichiometry? Global Biogeochemical Cycles, 29(9), 1369–1383. https://doi.org/10.1002/2015GB005137

Chen, N., Peng, B., Hong, H., Turyaheebwa, N., Cui, S., & Mo, X. (2013). Nutrient enrichment and N P ratio decline in a coastal bay–river system in southeast China: The need for a dual nutrient (N and P) management strategy. Ocean & Coastal Management, 81, 7–13. https://doi.org/10.1016/j.ocecoaman.2012.07.013.

Dai, Y., Yang, S., Zhao, D., Hu, C., Xu, W., Anderson, D. M., Li, Y., Song, X.-P., Boyce, D. G., Gibson, L., Zheng, C., & Feng, L. (2023). Coastal phytoplankton blooms expand and intensify in the 21st century. *Nature*, *615*(7951), 280–284. https://doi.org/10.1038/s41586-023-05760-y

de Wit, M., Behrendt, H., Bendoricchio, G., Bleuten, W., & van Gaans, P. (2002). The contribution of agriculture to nutrient pollution in three European rivers, with reference to the European nitrates directive. In European Water Management Online EWA 2002. Hennef, Germany/Brussels, Belgium.

Diaz, R. J., & Rosenberg, R. (2008). Spreading Dead Zones and Consequences for Marine Ecosystems. Science, 321(5891), 926–929. https://doi.org/10.1126/science.1156401.

Edgar (2019). Emission database for global atmospheric research, 1970–2010 (https://edgar.jrc.ec.europa.eu/overview.php?v ¼ 431). Vol. 2019, Ispra.

Food and Agriculture Organization (2021). Aquaculture production 2000–2015. FISHSTAT Plus- Universal software for fishery statistical time series by Fisheries and Aquaculture Information and Statistics Service. Food and Agriculture Organization of the United Nations. Rome. https://www.fao.org/fishery/statistics/software/fishstat/en.

Fujimoto, N., Sudo, R., Sugiura, N., Inamori, Y., 1997. Nutrient-limited growth of Microcystis aeruginosa and Phormidium tenue and competition under various N:P supply ratios and temperatures. Limnology

and Oceanography 42, 250e256.
Glibert, P. M. (2020). Harmful algae at the complex nexus of eutrophication and climate change. Harmful Algae, 91, 101583. https://doi.org/10.1016/j.hal.2019.03.001.
Galloway, J. N., Dentener, F. J., Capone, D. G., Boyer, E. W., Howarth, R. W., Seitzinger, S. P., et al. (2004). Nitrogen cycles: Past, present, and future. Biogeochemistry, 70, 153–226
Hallegraeff, G. M. (1993). A review of harmful algal blooms and their apparent global increase. Phycologia, 32(2), 79–99. https://doi.org/10.2216/i0031-8884-32-2-79.1.
Heisler, J., Glibert, P., Burkholder, J., Anderson, D., Cochlan, W., Dennison, W., Gobler, C., Dortch, Q., Heil, C., Humphries, E., Lewitus, A., Magnien, R., Marshall, H., Sellner, K., Stockwell, D., Stoecker, D., & Suddleson, M. (2008). Eutrophication and Harmful Algal Blooms: A Scientific Consensus. Harmful Algae, 8(1), 3–13. https://doi.org/10.1016/j.hal.2008.08.006.
Karlson, B., Andersen, P., Arneborg, L., Cembella, A., Eikrem, W., John, U., West, J. J., Klemm, K., Kobos, J., Lehtinen, S., Lundholm, N., Mazur-Marzec, H., Naustvoll, L., Poelman, M., Provoost, P., De Rijcke, M., & Suikkanen, S. (2021). Harmful algal blooms and their effects in coastal seas of Northern Europe. Harmful Algae, 102, 101989. https://doi.org/10.1016/j.hal.2021.101989.
Li, D. X., Gao, Z. Q., and Song, D. B., 2021. Analysis of environmental factors affecting the large-scale long-term sequence of green tide outbreaks in the Yellow Sea. Estuarine Coastal and Shelf Science, 260: 107504.
Marshall, H.G., Lane, M.F., Nesius, K.K., Burchardt, L., 2009. Assessment and significance of phytoplankton species composition within Chesapeake Bay and Virginia tributaries through a long-term monitoring program. Environmental Monitor Assess 150,143–155.
Morée, A. L., Beusen, A. H. W., Bouwman, A. F., & Willems, W. J. (2013). Exploring global nitrogen and phosphorus flows in urban wastes during the twentieth century. Global Biogeochemical Cycles, 27, 836–846. https://doi.org/10.1002/gbc.20072.
Ning, X.R., Lin, C.L., Su, J.L., Liu, C.G., Hao, Q., Le, F.F., Tang, Q.S., 2010. Long-term environmental changes and the responses of the ecosystems in the Bohai Sea during 1960–1996. Deep-Sea Res. II Top. Stud. Oceanogr. 57 (11), 1079–1091.
Páez-Osuna F (2001) The environmental impact of shrimp aquaculture: a global perspective. Environ Pollut 112:229–231. doi:10.1016 S0269-7491(00)00111-1.
Painting, S.J., Devlin, M.J., Malcolm, S.J., Parker, E.R., Mills, D.K., Mills, C., Tett, P., Wither, A., Burt, J., Jones, R., Winpenny, K., 2007. Assessing the impact of nutrient enrichment in estuaries: susceptibility to eutrophication. Marine Pollution Bulletin 55, 74e90.
Rabalais, N. N., Turner, R. E., & Wiseman, W. J. (2002). Gulf of Mexico Hypoxia, a.k.a. “The Dead Zone.” Annual Review of Ecology and Systematics, 33, 235–263.
Stehfest, E., van Vuuren, D. P., Kram, T., & Bouwman, A. F. (2014). Integrated assessment of global environmental change with IMAGE 3.0. In Model description and policy applications. The Hague: PBL Netherlands Environmental Assessment Agency. Retrieved from http://themasites.pbl.nl/models/image/index.php/Main_Page.
Tang, Q., Jin, X., Wang, J., Zhuang, Z., Cui, Y., Meng, T., 2003. Decadal-scale variations of ecosystem productivity and control mechanisms in the Bohai Sea. Fish. Oceanogr. 12 (4/5), 223–233.
Thomas Y, Courties C, Helwe YE, Herbland A, Lemonnier H (2010) Spatial and temporal extension of eutrophication associated with shrimp farm wastewater discharges in the New Caledonia Lagoon. Mar Pollut Bull 61:387–39doi:10.1016/j.marpolbul.2010.07.005
Van Beek, L. P. H., Wada, Y., & Bierkens, M. F. P. (2011). Global monthly water stress: 1. Water balance and water availability. Water Resources Research, 47, W07517. https://doi.org/10.1029/2010WR00979.
Van Dingenen, Rita, Frank Dentener, Monica Crippa, Joana Leitao, Elina Marmer, Shilpa Rao, Efisio Solazzo, and Luana Valentini. “TM5-FASST: A Global Atmospheric Source–Receptor Model for Rapid Impact Analysis of Emission Changes on Air Quality and Short-Lived Climate Pollutants.” Atmospheric Chemistry and Physics 18, no. 21 (November 13, 2018): 16173–211. https://doi.org/10.5194/acp-18-16173-2018.
Van Puijenbroek, P. J. T. M., Beusen, A. H. W., & Bouwman, A. F. (2019). Global nitrogen and phosphorus in urban waste water based on the shared socio-economic pathways. Global Environmental Change, 231, 446–456.
Vaquer-Sunyer, R., & Duarte, C. M. (2008). Thresholds of hypoxia for marine biodiversity. Proceedings of the National Academy of Sciences, 105(40), 15452–15457.

https://doi.org/10.1073/pnas.0803833105.
Wang, B.D., 2006. Cultural eutrophication in the Changjiang (Yangtze River) plume: history and perspective. Estuar. Coast. Shelf Sci. 69, 471–477.
Wang, H., Bouwman, A. F., Van Gils, J., Vilmin, L., Beusen, A. H. W., Wang, J., Liu, X., Yu, Z., & Ran, X. (2023). Hindcasting harmful algal bloom risk due to land-based nutrient pollution in the Eastern Chinese coastal seas. Water Research, 231, 119669. https://doi.org/10.1016/j.watres.2023.119669.
Wang, J., Bouwman, A. F., Liu, X., Beusen, A. H. W., Van Dingenen, R., Dentener, F., Yao, Y., Glibert, P. M., Ran, X., Yao, Q., Xu, B., Yu, R., Middelburg, J. J., & Yu, Z. (2021). Harmful Algal Blooms in Chinese Coastal Waters Will Persist Due to Perturbed Nutrient Ratios. Environmental Science & Technology Letters, 8(3), 276–284. https://doi.org/10.1021/acs.estlett.1c00012.
Wang, J., Beusen, A.H.W., Liu, X., Van Dingenen, R., Dentener, F., Yao, Q., Xu, B., Ran, X., Yu, Z., Bouwman, A.F. (2020a). Spatially explicit inventory of sources of nitrogen inputs to the Yellow Sea, East China Sea and South China Sea for the period 1970-2010. Earth's Future, 8, e2020EF001516. https://doi.org/10.1029/2020EF001516.
Wang, J., Beusen, A. H. W., Liu, X., & Bouwman, A. F. (2020b). Aquaculture Production is a Large, Spatially Concentrated Source of Nutrients in Chinese Freshwater and Coastal Seas. Environmental Science & Technology, 54(3), 1464–1474. https://doi.org/10.1021/acs.est.9b03340.
Wang, J.H., Wu, J.Y., 2009. Occurrence and potential risks of harmful algal blooms in the East China Sea. Sci. Total Environ. 407, 4012–4021
Xiao, M., Song, W., Zhang, H., Shi, X., & Su, R. (2024). Eutrophication of Jiangsu Coastal Water and Its Role in the Formation of Green Tide. Journal of Ocean University of China, 23(1), 109–118. https://doi.org/10.1007/s11802-024-5507-2
Xiao, X., Agustí, S., Pan, Y., Yu, Y., Li, K., Wu, J., & Duarte, C. M. (2019). Warming amplifies the frequency of harmful algal blooms with eutrophication in Chinese coastal waters. Environmental Science & Technology, 53(22), 13,031–13,041.
Yu, R. C., and Liu, D. Y., 2016. Harmful algal blooms in the coastal waters of China: Current situation, long-term changes and prevention strategies. Bulletin of Chinese Academy of Sciences, 31 (10): 1167-1174.
Yu, R. C., Liu, D. Y., and Liang, Y. B., 2018. Harmful algal blooms in the coastal waters of China. Global Ecology and Oceanography of Harmful Algal Blooms, 14: 309-316.
Zhou, K., Xu, Y., Kao, S.-J., Xiu, P., Wan, X., Huang, B., Liu, X., Du, C., Sun, J., Sun, Z., & Dai, M. (2023). Changes in nutrient stoichiometry in responding to diatom growth in cyclonic eddies. Geoscience Letters, 10(1), 12. https://doi.org/10.1186/s40562-023-00269-8.

Master Earth Science

Statement of originality

I declare that:

1. this is an original report, which is entirely my own work,
2. where I have made use of the ideas of other writers, I have acknowledged the source in all instances,
3. where I have used any diagram or visuals I have acknowledged the source in all instances,
4. this report has not and will not be submitted elsewhere for academic assessment in any other academic course. Student data: Name: Registration number: Date: Signature:

Student data:

Name: Fatemeh Afsari

Registration number: 2256424

Student Signature

Date: 31-05-2024 **Signature:** Fatemeh Afsari